



This is to certify that the  
thesis entitled

MOLECULAR IDENTIFICATION OF PATHOGENS IN ANCIENT  
SKELETAL REMAINS FROM BUTRINT AND DIAPORIT ALBANIA

presented by

Michael Joseph Mutolo

has been accepted towards fulfillment  
of the requirements for the

    M.S.     degree in     Forensic Science    



Major Professor's Signature

    12/12/06    

Date

*MSU is an Affirmative Action/Equal Opportunity Institution*

LIBRARY  
Michigan State  
University

**PLACE IN RETURN BOX** to remove this checkout from your record.  
**TO AVOID FINES** return on or before date due.  
**MAY BE RECALLED** with earlier due date if requested.

DATE DUE	DATE DUE	DATE DUE
APR 22 2010 540 410		

**MOLECULAR IDENTIFICATION OF PATHOGENS IN  
ANCIENT SKELETAL REMAINS FROM BUTRINT AND DIAPORIT ALBANIA**

**By**

**Michael Joseph Mutolo**

**A THESIS**

**Submitted to  
Michigan State University  
in partial fulfillment of the requirements  
for the degree of**

**MASTERS OF SCIENCE**

**School of Criminal Justice**

**2006**

## ABSTRACT

### MOLECULAR IDENTIFICATION OF PATHOGENS IN ANCIENT SKELETAL REMAINS FROM BUTRINT AND DIAPORT ALBANIA

By

Michael Joseph Mutolo

Paleopathologists and anthropologists examine skeletal lesions to better understand diseases that afflicted ancient societies. Traditional analyses of skeletal remains have limited success in identifying the particular organism or pathogen responsible. These limitations can be overcome by the addition of molecular techniques to screen for pathogen DNA present in the remains. Analysis of skeletal material from a World Heritage Site in Butrint and Diaporit, Albania demonstrated that pathogen DNA analysis could be a useful tool to the study of ancient cultures. Bone samples were collected from five sets of remains that showed pathologies, three late Roman (5<sup>th</sup> – 7<sup>th</sup> century AD) and two from the late Medieval period (11<sup>th</sup> – 13<sup>th</sup> century AD). Skeletal lesions seen in these remains had commonality indicating that the same pathogen may have been involved. In particular, lesions present on the vertebrae and ribs of the late Medieval samples were almost identical. Bone DNA extracts were screened for the presence of DNA from the causative agents of tuberculosis and brucellosis. Real-time PCR results indicated that the vertebrae and ribs of the late Medieval samples contained *Brucella spp.* DNA. This provides novel information on the ancient inhabitants of a culturally rich site that would have otherwise been unobtainable. This also represents the first time brucellosis has been molecularly identified in an ancient society and proved that molecular techniques can be used to investigate disease processes in other skeletal populations and cultures.

## TABLE OF CONTENTS

LIST OF TABLES .....	v
LIST OF FIGURES .....	vi
INTRODUCTION .....	1
Ancient Butrint, Albania.....	2
Ancient Diaporit, Albania.....	6
Anthropological Analysis of Skeletal Remains from Butrint and Diaporit.....	7
Skeletal Pathogens and their Identification through Traditional Methods .....	8
Tuberculosis Infection .....	11
Skeletal Tuberculosis Infection.....	12
Previous Osteological Studies of Skeletal Tuberculosis.....	13
Skeletal Brucellosis.....	15
Molecular Analysis of Ancient DNA .....	16
Ancient Pathogen DNA Analysis .....	18
Molecular Identification of Tuberculosis in Ancient Remains.....	19
Goal of this Project .....	21
MATERIALS AND METHODS.....	22
Description of Burials:.....	22
Bones Collected for Analysis.....	29
Bone Sample Preparation.....	32
Extraction of DNA.....	33
DNA Amplification using Polymerase Chain Reactions.....	34
Prevention of Contamination during Ancient DNA Analysis .....	37
Sensitivity Assays of the MTB Complex PCR Primers.....	38
Differentiation of <i>M. bovis</i> and <i>M. tuberculosis</i> .....	40
<i>M. tuberculosis</i> Mtp40 Primer Optimization and Primer Specificity Assays.....	41
Sequencing of Mitochondrial Hypervariable Region 1 .....	41
Real-Time PCR Primer Design for Tuberculosis, Brucella and Mitochondrial DNA ..	43
Optimization of Real-Time Primers.....	44
Real-Time PCR on Ancient Bone Samples .....	46
RESULTS .....	48
Bone Sample Preparation and DNA Extraction.....	48
MTB Complex Primer Optimization and Sensitivity Assays .....	49
Optimization of Methods used to Differentiate <i>M. tuberculosis</i> and <i>M. bovis</i> .....	51
Mtp40 Primer Specificity Assays .....	53
Screening of Bone Extracts for Tuberculosis DNA.....	54

Spiking Human Bone DNA Extracts with <i>M. tuberculosis</i> Genomic DNA.....	58
Mitochondrial DNA Amplification.....	59
Hypervariable Region I Sequencing .....	61
Real-Time PCR Optimization.....	64
Real-Time PCR Results of Voegtly Cemetery Samples.....	65
Real-Time PCR Results for Butrint and Diaporit Pathological Samples .....	70
 DISCUSSION .....	 83
Bone Preparation for DNA Extraction.....	84
DNA Extraction and PCR.....	86
Contamination and Ancient DNA Analysis.....	87
Human mtDNA Analysis to Assess the Quality of DNA in Skeletal Remains.....	89
Screening for Tuberculosis in Voegtly Cemetery Material using IS6110.....	92
Screening for Tuberculosis in the Voegtly Cemetery Material using OxyR and Mtp40 .....	93
Screening for Tuberculosis in Butrint and Diaporit Skeletal Material .....	95
Assessing Bones for Pathogen DNA using Real-Time PCR.....	97
Tuberculosis, Brucellosis, and Albania .....	100
 APPENDIX A.....	 107
 BIBLIOGRAPHY.....	 109

## LIST OF TABLES

Table 1: Description of Individual Burials .....	23
Table 2: Butrint and Diaporit Control and Livestock Samples.....	30
Table 3: Voegtly, Butrint and Diaporit Pathological Bone Samples .....	31
Table 4: Primer Sequences and Parameters .....	36
Table 5: Calculation of <i>M. tuberculosis</i> and <i>M. bovis</i> Genome Weight .....	39
Table 6: Real-Time PCR Primers .....	44
Table 7: Combination of Concentrations Used for Primer Optimization.....	45
Table 8: Summary of Analysis Conducted on Pathology and Questioned Bones.....	47
Table 9: Minimum Number of Genomic Copies Detectable .....	51
Table 10: Control/Livestock Extracts and IS6110 Experiments.....	55
Table 11: Questioned Pathological Samples and IS6110 Experiments.....	56
Table 12: Ranges of HV1 Sequence Obtained for each Bone .....	62
Table 13: Consensus Sequences Derived from Bone Samples for Pathogen Burials.....	63
Table 14: Optimum Primer Concentration and Average Ct Values for Primer Pairs.....	64
Table 15: Summary of Real-Time Results for Voegtly Burial 32 Rib mtDNA .....	69
Table 16: Summary of Real-Time Results for Voegtly Burial 32 Rib IS6110.....	69
Table 17: Summary of Real-Time Results.....	77
Table 18 (a – f): Ct Values and Tm for MtDNA Positive Reactions.....	78
Table 19 (a – e ): Ct Values and Tm for IS6501 Positive Reactions .....	80
Table 20 (a – b): Ct Values and Tm for Bcsp31 Positive Reactions .....	82
Table 21: HV1 Sequences from Individual Bone Samples. ....	107



## LIST OF FIGURES

Figure 1: Maps Depicting the Location of Butrint .....	3
Figure 2: Archaeological Sites of Butrint .....	5
Figure 3: Archaeological Sites of Diaporit .....	6
Figure 4: Butrint and Diaporit Pathological Descriptions and Photographs .....	24
Figure 5: Location of Albanian Burials .....	28
Figure 6: Variability of Aqueous Layers .....	48
Figure 7: Primer Sensitivity of IS6110 on <i>M. tuberculosis</i> DNA Dilutions.....	50
Figure 8: Differentiation of <i>M. bovis</i> from other Members of the MTB Complex .....	52
Figure 9: Mtp40 Specificity .....	53
Figure 10: PCR Screening for the Presence of IS6110 in Voegtly Samples .....	54
Figure 11: Screening of Vertebrae Samples for IS6110 using Nested PCR.....	57
Figure 12: IS6110 PCR on Bone DNA Extracts Spiked with <i>M. tuberculosis</i> DNA.....	58
Figure 13: Semi-Nested HV1 Results using DNA Extracted from Long Bones.....	59
Figure 14: HV1 Semi-Nested PCR of Vertebrae Extracts.....	60
Figure 15: MtDNA Amplication Plot for Voegtly Burial 32 Rib .....	66
Figure 16: MtDNA Dissociation Curve for Voegtly Burial 32 Rib .....	67
Figure 17: IS6110 Dissociation Curve for Voegtly Burial 32 Rib .....	68
Figure 18: MtDNA Amplification Plot for 4015 Vertebra .....	72
Figure 19: MtDNA Dissociation Curve for 4015 Vertebra .....	73
Figure 20: Real-Time IS6501 Amplification Plot for 4015 Vertebra.....	74
Figure 21: Real-Time IS6501 Dissociation Curve for 4015 Vertebra.....	75

~~SECRET~~

2

2007



Figure 22: Agarose Gel of Real-Time PCR Pathogen Results for 4015 Vertbra ..... 76

REFS

2

2007



## INTRODUCTION

Throughout history a number of diseases and pathogens have plagued mankind. Epidemics of cholera, small pox, bubonic plague, malaria and tuberculosis have spread rapidly through various ancient and modern civilizations. In the 14<sup>th</sup> century over twenty-five million Europeans died from the bubonic plague (Zivanovic 1982). In the 19<sup>th</sup> century the number one cause of death for working class citizens in the United States was tuberculosis (Zivanovic 1982). Past civilizations' interactions with these pathogens have created a desire in modern scientists to understand how epidemics directly impact today's societies.

Paleopathologists and physical anthropologists attempt to understand not only the manifestation of diseases in an individual, but also how diseases affect an entire society. Paleopathology involves the study of ancient human and animal remains for evidence of disease. Zimmerman and Kelly (1982) described multiple goals of paleopathology. The first is to understand how a pathogen has spread throughout a particular society and how the society's reaction to the epidemic has evolved over time. By studying an ancient society's response to disease, paleopathologists hope to understand how modern pathogens would behave in future epidemics. Another goal is to identify which diseases were present in a society by examining the characteristic lesions and markings left on mummified and skeletal tissue. This final goal is also important to physical and forensic anthropologists who attempt to identify abnormalities and pathologies in their analysis of human skeletal remains.

## *Ancient Butrint, Albania*

Zickel and Iwaskiw (1994) discussed the complex history of Albania and the struggles to preserve its culture. In 1944 the communist government took control of Albania and banned other nations, including the United States and Great Britain, from entering the country. As a result, the United States and nations of Western Europe had only limited knowledge of the culture and history of Albania. In the 1970s the United Nations Education, Science, and Cultural Organization (UNESCO) designated several locations in Albania as World Heritage sites. However, due to entrance restrictions imposed by the communist regime, archaeological and historical investigations were limited to scientists employed by the Albanian government. In the 1990s, the communist regime ended and scientists from other countries were once again allowed to enter the region. These scientists brought with them new research ideas and began the excavation of historical sites in conjunction with the Butrint Foundation, Packard Humanities, and the Albanian Institute of Archeology (Butrint Foundation Website). A joint report issued by UNESCO and the International Council on Monuments and Sites in 1997 stated that many of the historical sites had been looted and artifacts were destroyed. This report called upon scientists worldwide to aide in the preservation of ancient sites throughout Albania.

One historical site that was of particular interest was the ancient city of Butrint. Butrint is seated in the 'cradle of Western civilization' between Greece, Italy, former Yugoslavia, and the Adriatic Sea (Figure 1(a)). The city is located on a small peninsula of marshland in the southwest coast of Albania and is surrounded by three bodies of water including Lake Butrint, an inland lagoon, and a series of straits (Figure 1(b)).

**Figure 1: Maps Depicting the Location of Butrint**

(a). Location of Albania in relation to other southeastern European countries and the Adriatic Sea. (b). The city of Butrint (red box) in relation to surrounding bodies of water.



(Butrint Foundation Website)

The Butrint Foundation has published several reports on the history of the ancient city (UNESCO 1999). Over the ages the site of Butrint has been inhabited by a number of different cultures including Greeks, Romans, Byzantines, and Venetians. The Greek Chaonian Tribe first founded the city in the 8th century BC. By the 4<sup>th</sup> century BC the site was dedicated to Aesclepius, the Grecian God of Medicine, and had taken on the appearance of a Greek polis with temples, theaters, and public buildings. In 44 BC the city was seized by the Roman Empire and became part of the Illyrian province. Butrint expanded considerably under Roman control, and eventually was made a diocese of a

bishop during the height of early Christianity. This period also marked the construction of Roman infrastructure, such as roads and aqueducts. The city played a vital role as a port for the Roman Empire and a diverse assemblage of peoples (European, Middle Eastern and African) are believed to have used the site as a trade route.

Butrint began to decay in the 5<sup>th</sup> and 6<sup>th</sup> centuries when the collapse of the Roman Empire caused infrastructure failure (UNESCO 1999). A Slavic invasion in the 7<sup>th</sup> century AD led to abandonment of the city, but the site regained its prosperity under the Byzantine administration during the 9<sup>th</sup> century. Little is known about the city following this period until it came under Venetian control in 14<sup>th</sup> century AD. Power struggles between the Venetians and Ottoman Turks continued for several centuries. In the late Middle Ages waters from the marsh and surrounding lakes flooded the city leading to its ultimate abandonment.

Butrint has been well characterized archaeologically (UNESCO 1999). Four sites have been excavated and are currently being studied and preserved by the Albanian Institute of Archeology (Figure 2). The majority of the archaeological work has been conducted on the Triconch palace that sits near the shore of the Adriatic Sea. This palace was believed to have reached its peak use during the 4<sup>th</sup> and 5<sup>th</sup> centuries AD. It was abandoned during the 6<sup>th</sup> and 7<sup>th</sup> centuries but later was re-occupied by the Venetians. Other sites of interest include a Greek amphitheatre and an early Christian baptistery.



**Figure 2: Archaeological Sites of Butrint**

Photograph (a) depicts an aerial view of the archaeological sites and ancient city of Butrint (Butrint Foundation Website). Photograph (b) is an image of the early Christian Baptistery (Murray 2005). Photograph (c) depicts an image of the Triconch palace while (d) is the Greek amphitheater (Murray 2005 and Butrint Foundation Website).

(a).



(b).



(c).



(d).



### *Ancient Diaporit, Albania*

On the eastern shores of Lake Butrint sits an additional archaeological site known as Diaporit (Figure 3). Archeological evidence suggests that this site was first occupied during the late 3<sup>rd</sup> century BC when a small villa was established (Butrint Foundation Annual Report 2004). The Romans first entered the area in the early 1<sup>st</sup> century AD and from 50 to 80 AD established a large villa. Excavations have revealed several features of this Roman villa including fountains, courtyards, elaborate mosaics, and a roman bathhouse. Archeological evidence of mosaics and a church indicates that Christianity arrived to the area between the 5<sup>th</sup> and 7<sup>th</sup> century AD.

#### **Figure 3: Archaeological Sites of Diaporit**

Map depicted in (a) shows the location of Diaporit in relation to other excavation sites currently being studied in Albania (Butrint Foundation Annual Report 2004). Photograph (b) is of the excavated Roman Villa (Fenton 2006).

(a).



(b).



### 3.2.2.2. *Phragmites australis*

#### 3.2.2.2.1. *Phragmites australis*

##### 3.2.2.2.1.1. *Phragmites australis*

174



## *Anthropological Analysis of Skeletal Remains from Butrint and Diaporit*

Excavations of the Butrint and Diaporit sites led to the discovery of several burials, which remained uninvestigated until very recently. Dr. Todd Fenton and graduate students from Michigan State University conducted anthropological analysis to characterize the inhabitants of the sites. Skeletal remains were analyzed to access the individuals' age and sex. According to the Butrint Foundation's 2004 annual report Fenton and his students had thus far completed skeletal analysis on 80 individuals from the Diaporit site and 105 from Butrint. Bone samples from a number of skeletons were collected and brought to Michigan State University for molecular analysis.

Some of these individuals displayed skeletal lesions that may be associated with pathologies such as tuberculosis or brucellosis. Both diseases have been identified in ancient and modern day Albanian societies (World Health Organization 2000). It is believed that the Roman Empire's collapse, combined with failure of infrastructures and conflicts over the region enhanced societal decay (Butrint Foundation Annual Report 2004). Poor living conditions, lack of resources, and the introduction of foreign cultures could have led to the spread of disease and epidemics, which expedited this process

## *Skeletal Pathogens and their Identification through Traditional Methods*

According to Zimmerman and Kelley (1982), the characterization of pathogens in human skeletal remains can be a challenging process. Many pathogens that are able to infect bone do not lead to the manifestation of skeletal abnormalities or lesions. Lack of these skeletal lesions is believed to be a result of rapid recovery or death immediately following infection. Furthermore, if abnormalities or skeletal lesions are produced they are rarely distinctive enough to identify the particular organism causing the disease. Long term or chronic infection is usually required for the manifestation of skeletal lesions.

Zimmerman and Kelley (1982) described two broad categories of bone infection: pyogenic and granulomatous. Pyogenic organisms such as staphylococci and streptococci cause infections that result in pus formation. These organisms can infect any bone in the body, producing inflammation in the marrow, cortex, and periosteum. Pyogenic infections of bone typically arise from bacteria in the blood stream or as an outgrowth of soft tissue. Once localized in bone, the infection can become chronic without medical treatment. Infected bone may display an irregular thickened appearance and numerous cloacae (channels or holes through the cortex). Pyogenic lesions are characterized by bone erosion with sequestra (small areas of new bone regeneration).

Granulomatous organisms produce pockets of infection that contain masses of bacterial cells and host leukocytes. Examples include the pathogens that cause leprosy, tuberculosis, syphilis and some fungal infections. These organisms can infect any bone

in the body, resulting in areas of erosion. In contrast to pyogenic infection, granulomatous organisms erode bone while inhibiting sequestra or bone regeneration.

Ortner and Putschar (1981) described some of the traditional methods used by paleopathologists and anthropologists to study skeletal lesions, including gross analysis, X-ray examination, chemical analysis, and microscopic examination. Gross and X-ray analyses involve the examination of skeletal material to provide a description and understanding of the disease process that causes skeletal abnormalities. Anthropologists use these methods to identify the number of lesions present and describe the overall appearance and quality of the bone tissue. Identification of abnormalities and their distribution throughout the skeleton can provide further information on the disease and its manifestation.

Microscopic and chemical based methods tend to be more limited than gross or X-ray analyses. Chemical tests detect the levels of certain amino acids and minerals, such as fluorides and iron, in bone tissue. Von Endt and Ortner (1982) used amino acid analysis to identify potential anemia caused by malnutrition in the skeletal remains of American Southwest Pueblo Indians. Bone proteins in children that showed signs of skeletal anemia had 25% less amino acids that contained hydroxyl groups (serine, threonine, and tyrosine) and acidic-side chains (aspartic and glutamic acid) compared to children who had died from trauma. Enzymes that require an iron co-factor synthesize these amino acids. Based on their test results, Von Endt and Ortner (1982) hypothesized that the children were experiencing anemia due to iron deficiencies caused by a limited diet.

Microscopy, or histological analysis, relies on examination of osteoblasts and osteoclasts. Osteoblasts are cells that secrete bone, while osteoclasts remove portions causing the production of the bone matrix. Paget's disease is an example of a metabolic bone abnormality that can be identified using microscopy. This disease simultaneously causes an increase in osteoclast and osteoblast activity, resulting in a bone matrix that appears fragmented when viewed microscopically.

These traditional techniques are limited and directly influenced by the condition of the skeletal remains and bone samples being studied (Ortner and Putschar 1981). Highly fragmented material may be difficult to examine, and understanding how pathologies affect the skeleton as a whole is nearly impossible. Microorganisms found in soil can also damage bone tissue, creating abnormalities that are similar to disease processes. One way to surpass these limitations is to combine skeletal examination with molecular genetic techniques.

Several published articles have described the identification of pathogen DNA in ancient human remains. It is believed the presence of pathogen DNA in bone could indicate either acute or chronic infection during an individual's lifetime. Past genetic analysis of ancient DNA has proved successful in identifying the presence of a wide range of pathogens, including malaria, leprosy, plague, tuberculosis, and syphilis in a number of ancient societies (Rafi et al. 1994, Drancourt and Raoult. 2004, Sallares and Gomzi. 2001, Hunnis 2004, Mays et al. 2002).

## *Tuberculosis Infection*

Despite progress in modern healthcare, medicine, and improved living standards, tuberculosis is still one of the most common diseases, killing an average of 1.7 million people a year worldwide (WHO 2006). The disease is caused by the infection of lung or soft tissue by small, acid fast, gram-positive bacteria. These bacteria are members of the Mycobacterium Tuberculosis Complex (MTB complex), which includes a number of pathogenic Mycobacterium species (*M. bovis*, *M. tuberculosis*, *M. microtti*, *M. africanus*, etc.) and infect a wide range of hosts. The disease in humans is primarily caused by *M. tuberculosis* or *M. bovis*.

Mays et al. (2002) and other authors have summarized the history of tuberculosis. *M. bovis* is thought to be the primary infectious organism that inflicted ancient societies. It is transmitted by the inhalation of contaminated aerosol from livestock or through the ingestion of contaminated meat or milk. Ingestion of the bacterium results in foci or small nodules of infection in the intestinal walls and lymph nodes. Since the 19th century the majority of tuberculosis cases have been caused by the spread of *M. tuberculosis* from person to person through the inhalation of contaminated aerosol. Industrialized and Western societies are particularly hard hit by the disease since its spread seems to be dependent on population-density. Once the organism is inhaled, pulmonary infection ensues by the formation of foci in the lung. The foci, if not healed by the individuals' immune system, will progress, spreading first to surrounding lymph nodes and then to the blood stream. The spread of bacteria to the blood stream can result in secondary infection of soft, skeletal, and organ tissue. The degree of secondary infection is highly



dependent on the virulence of the organism, the size of the inoculum, and the resistance level of the individual's immune system.

### *Skeletal Tuberculosis Infection*

Ortner and Putschar (2001) characterized the infection of the skeleton and bone tissue by tuberculosis bacilli. Skeletal manifestations of the disease are more common in unhealthy adults and young children. It is estimated that 50 to 90 percent of cases of tuberculosis occur in individuals between 3 and 15 years of age. Skeletal lesions may begin to develop at this time and usually persist well into adulthood. It is estimated that only 5 to 7 percent of skeletal tuberculosis infections result in lesion production (Zimmerman and Kelley 1982). However, this number may be an underestimate due to the variability and expression of lesions. One of the difficulties in diagnosing tuberculosis in skeletal populations is that there are no absolute criteria for osteological identification.

The most common site of skeletal tuberculosis infection is the spinal column and vertebrae (Ortner and Putschar 2001). The part of the spinal column involved is almost exclusively the vertebral bodies; while involvement of the vertebral arches is rare. It is believed that the bacilli travel through the blood stream, up the paravertebral plexus and attack the center, the anterior surface, or the paradiscal region of the vertebral body. Uehlinger (1970) conducted a study on 62 individuals that had been diagnosed with tuberculosis at autopsy. He found that the most common vertebrae involved were thoracic (particularly T6 – T12) and lumbar (L1 – L5). Vertebral infections are lytic and

produce lesions that Mays et al. (2002) described as circular resorptions present on the anterior surface of the vertebrae. The bacteria will continue to cause these lesions and destruction until the vertebrae collapse. Vertebral collapse caused by tuberculosis, also known as Pott's disease, is characterized by "kyphosis", or angling of the vertebral column followed by fusion of the spine.

Zimmerman and Kelley (1982) reported that weight-bearing joints could also become infected with tuberculosis. The bacilli enter the joint from adjacent bone or tissue membranes that line the surrounding areas. Once situated in the joint, the bacteria erode bone tissue creating lesions on articulating surfaces. Extra-vertebral tuberculosis has also been found to affect ribs as well as bones of the limbs, skull and pelvis.

#### *Previous Osteological Studies of Skeletal Tuberculosis*

Kelley and El-Najjar (1980) examined the natural variation and patterns of skeletal tuberculosis in the Hamann-Todd osteological collection. This collection contains approximately 500 individuals who demonstrate signs of tuberculosis infection. Twenty-six individuals were selected, using medical records or death certificates that documented them as suffering from skeletal tuberculosis. Gross and X-ray analyses were conducted to characterize the location and severity of the lesions. Their results indicated that the most common site of lesions was the lower spine (57.7%) from T11 to L5. The authors commented that 40 – 50% of the skeletons examined showed signs of tuberculosis in other bones. Rib involvement was the second most common site with 34.6% of individuals having lesions on the side of the rib facing the lungs or at the site of vertebral articulation. Skeletal tuberculosis was also noted in the pelvis, knee, sternum,

shoulder, clavicle, and femur. Thirty-eight percent of the individuals showed signs of tuberculosis infection in multiple bones.

Ortner and Putschar (1981) stated that rib lesions associated with tuberculosis are generally found in two locations: near the rib head (the portion of the rib that articulates with the vertebral body) or on the visceral surface (the posterior surface of the ribs that faces the lungs) due to the spread of overlying pulmonary foci. Kelley and Micozzi (1984) examined the association between rib lesions and pulmonary tuberculosis in the Hamann-Todd collection. Seventy individuals were selected that showed signs of skeletal tuberculosis. The authors reported that 55.7% of the skeletons examined contained evidence of lesions on the rib visceral surface. Based on these results they hypothesized that rib lesions could have been produced by adjacent pulmonary lesions. They concluded that there is a strong correlation between rib lesions and pulmonary tuberculosis in the Hamman-Todd Collection.

Roberts et al. (1994) conducted another study of tuberculosis rib infection by examining the Terry anatomical collection. Out of 255 documented tuberculosis cases, 62% showed visceral surface rib lesions. However, 22% of individuals that died from non-tubercular pulmonary diseases (i.e. pneumonia, bronchitis, emphysema) and 15% of individuals with non-pulmonary causes of death showed similar lesions. The authors concluded that visceral rib lesions are not a definitive indicator of pulmonary tuberculosis and could be associated with other pathogenic infections.

## *Skeletal Brucellosis*

There are several types of pathologies that can resemble skeletal tuberculosis, including secondary malignant bone tumors, fractures of the vertebrae, pyogenic osteomyelitis, Paget's disease, rheumatoid arthritis, brucellosis, and fungal infections (Kelley and El-Najar 1980). Ortner and Putschar (1981) described the infection of skeletal material by *Brucella spp.*; a gram-negative coccobacilla that causes the disease brucellosis. Three members of *Brucella spp.* are pathogenic to domestic livestock including *B. abortis*, *B. suis*, and *B. melitensis*. The latter two have also been associated with human infection and are primarily transmitted through ingestion of the bacteria. *B. melitensis* is common in goats and sheep from the Mediterranean and is transmitted through the ingestion of infected meat or milk products. Similarly, *B. suis* infects domestic swine and is transmitted through meat. *B. abortis*, a strain that can cause miscarriages in cattle and horses, may also infect humans in extremely rare cases.

Brucellosis in humans usually manifests as a chronic lung infection followed by recurring fevers. Skeletal tissue will become involved with chronic infection, especially with *B. melitensis*, and can vary from 2 – 70% of cases (Jaffe, 1972). Foci of the bacteria spread to cancellous bone from the bloodstream and produce skeletal lesions. Once in cancellous bone the foci will produce lytic cavities and the overlying cortex may become perforated with little evidence of healing. The vertebral column and pelvis are the most common sites of infection with each containing multiple foci. As a result the lesions produced appear very similar to those of skeletal tuberculosis. A major difference between tuberculosis and brucellosis infection is that *Brucella spp.* tend to be less

destructive than members of the MTB complex. As a result brucellosis does not cause severe degradation of joints or kyphosis of the vertebral column.

### *Molecular Analysis of Ancient DNA*

The analysis of ancient DNA can provide a vast amount of information about an individual and a society. In our laboratory, ancient DNA analysis has been used to study family groups, genetic diversity, human migration patterns, and ancestry (Clemmer 2005, Rennick 2005, Murray 2006). Data obtained from such studies can compliment anthropological analysis by providing novel information that would not otherwise be obtainable.

DNA extracted from ancient remains is often highly degraded and of low copy number. The amount of DNA template must be increased before genetic analysis can be conducted. Polymerase chain reaction (PCR) is a method used by molecular biologist to amplify small amounts of DNA. PCR involves the use of thermal cycling in which a sample of DNA is heated and cooled in a precise pattern in the presence of Taq DNA polymerase. This results in the amplification of a specific region of DNA sequence. The boundaries of the amplified sequence are defined by short pieces of DNA, known as oligonucleotide primers. Primers are designed so that they are complimentary to DNA sequences that flank the desired product (often termed the amplicon). This allows molecular biologist to target a particular DNA region of interest. Amplification of DNA using PCR is exponential: after 30 cycles, billions of copies of the target region can be produced from a very small amount of starting material. The sensitivity of PCR has been

greatly increased by the development of nested PCR. In this process, additional cycles are conducted on the amplified template using primers internal to those used in the first round. This allows for the amplification of extremely small amounts of starting template, such as those found in skeletal remains.

In ancient material, nuclear (chromosomal) DNA is often too degraded to analyze. Instead analysis of mitochondrial DNA is conducted. Mitochondria are organelles located in the cell that are responsible for producing energy. In humans, mitochondria contain a circular genome that is 16,569 bases in size. This genome has both protein coding and a non-coding segment; the latter is also known as the control region and is further divided into two hypervariable (HV) regions: HV1 and HV2. The non-coding nature of the hypervariable regions has allowed mutations to accumulate due to a lack of selection against them. As a result, unrelated individuals tend to contain on average 3% base differences (i.e. polymorphisms) in the DNA sequences of their HV regions (Hummel 2003). Polymorphisms have accumulated over time and are passed from generation to generation through maternal lineages. Maternal ancestors will share the same mtDNA sequence, termed a haplotype, which generally differs from sequences found in unrelated individuals. In forensic science, the sequences of mtDNA HV regions are compared to each other and to a reference sequence (Anderson et al. 1981) to identify remains as belonging to a family group. Previous studies in our laboratory have utilized PCR and mtDNA analysis on Albanian ancient skeletal material to look at genetic diversity and maternal relatedness of ancient individuals (Clemmer 2005, Murray 2006, Rennick 2005).

## *Ancient Pathogen DNA Analysis*

DNA analysis can aid in the identification of the specific pathogen that produced skeletal lesions. Pathogen DNAs may be preferentially amplified by designing primers that target sections of the pathogen's genome, without binding to any host sequences. Shawar (1993) described the use of PCR to identify members of the MTB complex in lung tissue and sputum from pathological samples. PCR was conducted to screen for the presence of a mobile genetic element, IS6110, which is found in the genome of MTB complex members. The copy number of IS6110 varies by species, with *M. tuberculosis* having 8 – 20 copies and other members of the complex having as few as one. Because it is unique to *Mycobacterium spp.*, amplification of IS6110 is a quick and reliable method to screen samples for a member of the MTB complex.

Other PCR based methods have been developed to differentiate members of the MTB complex. Most efforts have focused on differentiating *M. tuberculosis* and *M. bovis*. A method developed by Sreevatsan et al. (1996) involves the amplification of the OxyR gene to determine which base is present at position 285. All *M. bovis* strains contain an adenine (A) at this site, while all other MTB complex members contain a guanine (G). Screening for this conserved polymorphism has become a diagnostic tool for *M. bovis* infection.

Differentiating *M. tuberculosis* from other members of the MTB complex has proven more difficult because they share 95 – 99% genetic homology. Methods to identify *M. tuberculosis* as the pathogenic agent usually involve screening for species-specific genes, such as Mtp40. Parra et al. (1991) identified the Mtp40 gene as a 402 bp

segment of DNA that encodes a protein specific to *M. tuberculosis*. The absence of Mtp40 from other members of the MTB complex has allowed it to be utilized as a diagnostic tool for *M. tuberculosis* infection.

### *Molecular Identification of Tuberculosis in Ancient Remains*

While most of the assays described above were developed for modern samples, the methods have been modified to identify tuberculosis in ancient remains. In 2001, Mays et al. published a paper describing the use of PCR to screen for MTB complex DNA in nine human skeletons from the Wharton Perry Collection. Gross and X-ray analyses were used to characterize lesions on the vertebral bodies and joints of nine individuals. According to the authors skeletal lesions included “cavitations of the cancellous bone...with little new bone formation...” Spinal kyphosis and vertebral body collapse were also seen in several of the remains. Material was collected from the inside of lesions from each individual and from two control individuals. DNA extracted from this material was first screened for IS6110 using nested PCR. Bones from seven of the nine individuals resulted in a positive PCR reaction, indicating that a member of the MTB complex’s DNA was present. Further analysis of the OxyR and Mtp40 gene determined the infectious agent was *M. tuberculosis*.

Mays et al. (2002) continued this work by investigating the relationship between visceral rib lesions and tuberculosis. Ribs from the seven positive burials identified in the 2001 studies were screened along with ribs from seven burials that lacked rib lesions. IS6110 PCR products were obtained from one of the positive burials and two ribs from a



control burial. The authors concluded that rib lesions do not appear to be directly associated with tuberculosis infection in the Wharton Perry population. They also stated that molecular techniques could be used to detect pathological infection even when skeletal lesions are absent.

Mays et al.'s studies (2001 and 2002) were limited to the analysis of bones from a single collection. Zink et al. (2005) expanded this research by attempting to isolate MTB complex DNA from different skeletal populations. The first group included vertebrae from recent cases of systemic tuberculosis that were collected at autopsies conducted in Munich from 1990 – 2000. An additional 12 vertebral samples were collected as controls from individuals that died from other causes. Historical remains from a necropolis in Egypt (1550 – 500 BC) and a 14<sup>th</sup> century German cemetery were also tested. Egyptian bone samples consisted of vertebrae from 36 skeletons: 5 showing signs of tuberculosis, 12 showing pathologies of unknown origin, and 19 that appeared normal. The German cemetery sample set consisted of 51 long bones from skeletons that showed signs of thickening, porosity and periosteal reaction (morphological changes in bone surface).

In the modern group, 8 out of 12 cases tested positive for the MTB complex. Results obtained from the historical Egyptian collection varied in the degree of visible skeletal lesions. In total, 7 out of 36 vertebrae resulted in positive amplification of IS6110. This included 3 out of 5 that showed tuberculosis characteristic lesions, 2 out of 12 that showed unknown pathologies, and 2 out of 19 that appeared normal. Ten out of 51 of the German long bone samples tested positive. Zink et al. (2005) concluded that the use of IS6110 as a molecular tool for the identification of MTB complex DNA is feasible with both modern and ancient materials. They also concluded that molecular screening

techniques for pathogens can be informative in instances where skeletal lesions are minimal.

### *Goal of this Project*

The identification of pathogens in ancient and modern skeletal remains is of great interest to both paleopathologists and anthropologists. Molecular techniques have proven their ability to aid in identifying the specific organism responsible for skeletal lesions. This is accomplished by screening bone samples for the presence of pathogen DNA. The goal of this project was to utilize molecular techniques, such as PCR, SNP analysis, and real-time PCR, to analyze skeletal remains from the ancient cities of Butrint and Diaporit in present day Albania. An anthropological study of remains from these sites had identified several individuals that showed pathologies consistent with tuberculosis or brucellosis. Bone samples were screened for the DNA of pathogens that cause these diseases, the first time that such methods were applied to ancient skeletal remains from Albania. This research not only showed that molecular techniques could complement osteological analysis in the identification of pathogens, but also provides information on the lives and deaths of individuals that inhabited a culturally rich site.

## MATERIALS AND METHODS

### *Description of Burials:*

Bone samples from eleven human and three livestock skeletons were used in this study. Table 1 provides a summary of the location, time period, and biological profiles of the burials. Bones from two individuals, burials 32 and 629, originated from a cemetery in Pittsburgh, PA, and had previously tested positive for *M. tuberculosis* DNA in a study conducted by Ubelaker et al. (2003). The remaining nine individuals were from Butrint and Diaporit, Albania. Dr. Todd Fenton and graduate students divided the individuals into three categories: tuberculosis/brucellosis consistent, questioned pathologies, and controls. Individuals, 2722 and 4015 showed skeletal lesion whose appearance were consistent with previous reported cases of skeletal tuberculosis or brucellosis (Mays et al. 2002). The questioned pathology group consisted of skeletal remains from three burials, 213, 319 and 5010, which showed minimal damage or only contained a subset of the characteristic lesions described by Mays et al. (2002). Bones from four skeletons that contained no signs of pathologies were selected to serve as controls. More detailed information on the pathological burials for the Butrint and Diaporit sites are outlined in Figure 4.

**Table 1: Description of Individual Burials**

A description of remains sampled in this study. The information is arranged by categories assigned during osteological examination and the site where the burials were found. Time Period, Sex, and Age at Death information for the Voegtly cemetery burial was obtained from Uberlaker et al. (2003). Dr. Todd Fenton and graduate students provided information on the Albania burials. Date following 'Location' indicates the year in which the burial was excavated. Information was undetermined for some individuals (Undet).

Burial #	Location	Time Period	Sex	Age
<b>Voegtly Samples</b>				
32	Pittsburgh PA 1987	Late 18 <sup>th</sup> Century	Male	Adult
629	Pittsburgh PA 1987	Late 18 <sup>th</sup> Century	Female	Adult
<b>Control Samples</b>				
10	Diaporit 2000	Roman	Female	Undet
584	Diaporit 2002	Roman (5 <sup>th</sup> – 7 <sup>th</sup> Century)	Undet	Undet
3023	Butrint 2001	Medieval	Undet	Undet
3060	Butrint 2001	Medieval	Undet	Adolescent
<b>Questioned Samples</b>				
213	Diaporit	Roman (5 <sup>th</sup> – 7 <sup>th</sup> Century)	Male	Adult
319	Diaporit 2001	Roman (5 <sup>th</sup> – 7 <sup>th</sup> Century)	Female	Adult
5010	Butrint 2002	Roman (5 <sup>th</sup> – 7 <sup>th</sup> Century)	Female	Adult
<b>Suspected TB/Brucella Pathological Samples</b>				
2272	Butrint 1995	Medieval (11 <sup>th</sup> – 13 <sup>th</sup> Century)	Male	Adolescent
4015	Butrint 2002	Medieval	Male	Adolescent
<b>Livestock Samples</b>				
M5207	Butrint 2003	Late 5 <sup>th</sup> Century	Undet	Undet
M5267	Butrint 2003	Late 5 <sup>th</sup> Century	Undet	Undet
M5509	Butrint 2003	Late 5 <sup>th</sup> Century	Undet	Undet

#### **Figure 4: Butrint and Diaporit Pathological Descriptions and Photographs**

Descriptions of tuberculosis/brucellosis consistent and questioned pathology burials are provided. Images show examples of pathological lesions found on the skeletal remains. (Osteological data provided by Dr. Todd Fenton and his graduate students).

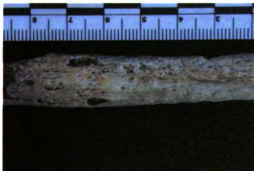
##### **(a) Individual 213:**

Skeletal remains of an adult male from Diaporit dated to the Roman era in the 5<sup>th</sup> – 7<sup>th</sup> Century AD. Pathologies included osteophytic lipping on lumbar vertebrae (left image) while cervical and thoracic vertebrae showed evidence of bony growths. The ulna contained poritic lesions and sclerotic bone at the proximal and distal ends (right image). The left femur and tibia (not shown) appeared expanded with sclerotic bone at both ends.



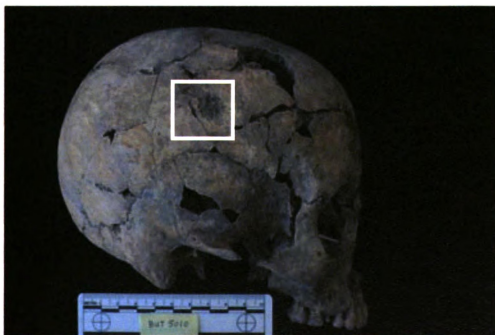
##### **(b) Individual 319:**

Skeletal remains of an adult female from Diaporit dated to the Roman era in the 5<sup>th</sup> – 7<sup>th</sup> Century AD. Pathologies included osteophytic lipping and porosity on cervical vertebrae, porosity of the ribs (left image), and lesions on the parietals of the skull (right image). Both tibiae and one fibula (not shown) displayed expansion and reactive woven bone.



**(c) Individual 5010**

Skeletal remains of an adult female dated to the Roman era in the 5<sup>th</sup> – 7<sup>th</sup> Century AD that were excavated from the Triconch Palace in Butrint. Porotic hyperostosis was seen throughout the skeleton. Oval and circular lesions were present on the frontal and parietal bones of the skull (area outlined by the white box). Cervical vertebrae showed osteophytic lipping and extensive periosteal reactions were noted on the humeri, femora, and tibia (not shown).



**(d) Individual 2272**

Medieval (11<sup>th</sup> – 13<sup>th</sup> Century AD) skeletal remains of an adolescent male excavated from the Baptistery in Butrint. Multiple circular lesions and areas of erosion were present on the thoracic vertebrae. Ribs showed signs of cortical expansion and the fibula showed some expansion of the metaphyses (not shown). The femoral shafts had myostosis ossifications and contained porosity and expansion of the head (not shown).



**(e) Individual 4015**

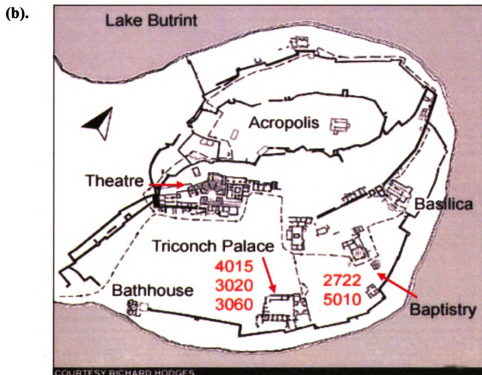
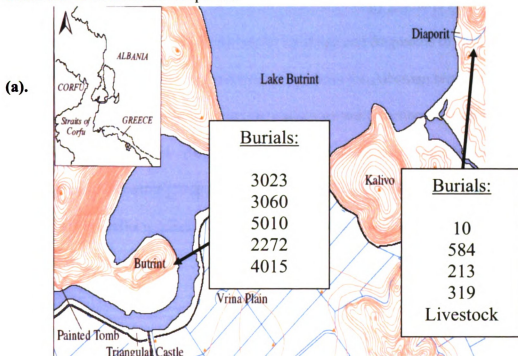
Medieval (11<sup>th</sup> – 13<sup>th</sup> Century AD) skeletal remains of an adolescent male excavated from the Merchant House in Butrint. Multiple circular lesions and areas of erosion were present on several thoracic vertebrae. Ribs showed thickening, orbicular expansion and lesions on the anterior surface with porosity on the visceral surface (not shown).





**Figure 5: Location of Albanian Burials**

(a). Distribution of burials by excavation site. (b). Site plan of Butrint with general position of burials marked in red. Burial 2722 was found near the baptistry. 5010 was located inside the Triconch palace. 4015, 3023, 3060 were found inside the merchant house that is located near the palace.



### *Bones Collected for Analysis*

The Voegtly cemetery samples from burials 32 and 629 consisted of fragmented ribs and femur cross-sections (Table 3). A forensic biology graduate student from Michigan State University collected whole vertebrae and fragments of ribs, pelvises, skulls, metacarpals, metatarsals, and long bones from the Albanian remains (Murray 2005). Larger bones that showed signs of pathology were sectioned using a Dremel tool fitted with a cutting wheel. Butrint and Diaporit bone samples available for DNA analysis from the control group and livestock remains are outlined in Table 2. The tuberculosis/brucellosis consistent and questioned bones are outlined in Table 3.

**Table 2: Butrint and Diaporit Control and Livestock Samples**

Bones samples collected for DNA analysis are listed and arranged by burial number.

Burial Number	Bone Sample
10	Thoracic Vertebrae
	Left Rib
	Fibula
	Tibia
	Metacarpal
584	Thoracic Vertebrae
	Pelvis
	Left Rib
	Femur
	Radius
	Metatarsal
M5207	Ulna
	Calcanium
M5267	Vertebrae
M5509	Ulna
	Rib
	Phalanx
	Radius

**Table 3: Voegtly, Butrint and Diaporit Pathological Bone Samples**

Bones collected for DNA analysis and brief description of pathologies noted by Ubelaker et al. (2003) (indicated by \*) or Fenton (2006) arranged by burial number.

Burial Number	Bone Sample	Pathologies Described During Osteological Analysis
32*	Rib	Lesions on Cervical Vertebrae
	Femur	
629*	Rib	Ossified nodules and lesions on Vertebrae
213	Thoracic Vertebrae	Adjacent to Three Vertebrae that Showed Pathology
	Ischium	Small Amount of Pathology
	Femur	-
	Ulna	Lesion on
	Fibula	Pathology on Distal End
	Metacarpal	-
319	Thoracic Vertebrae	-
	Rib	Ribs show signs of Porosity
	Femur	-
	Fibula	Shows signs of Pathology on Distal Half
	Skull	Shows signs of Pathology
	Ulna	-
	Metacarpal	-
5010	Thoracic Vertebrae	
	Rib	Skeletal lesions on Multiple Ribs
	Femur	-
	Fibula	-
	Humerous	Skeletal lesions present
	Metacarpal	-
4015	Thoracic Vertebrae	Multiple circular lesions on the anterior
	Rib	Rib thickening and trabecular expansion; minor porosity visceral surface
	Femur	-
	Pelvis	-
	Metacarpal	-
2272	Thoracic Vertebrae	Multiple circular lesions on the anterior
	Rib	Most ribs exhibit cortical expansion
	Pelvis	
	Radius	-
	Fibula	Expansion of metaphysis
	Metacarpal	-
	Femur	Porosity on femoral neck; expansion of distal metaphyses

### *Bone Sample Preparation*

Digestion buffer (50 mM EDTA, 0.5% SDS, 20 mM Tris pH 8.0), bone wash solution (10 mM EDTA, 0.5% SDS, 20 mM Tris pH 8) and water were sterilized by passing them through a 0.22-micron filter. A Dremel tool, drill parts, rotary tool, sanding wheel, 1/16 inch drill bits, weigh paper, weigh boats, sterile 1.5 mL microcentrifuge tubes, and filtered liquids were UV irradiated at 6 joules per cm<sup>2</sup> for 5 minutes.

Bones were cleaned and prepared for sampling in a UV sterilized Cleanspot Workstation. For whole bone and large bone fragments (e.g., a whole vertebra or large section of femur) a small portion of the surface was prepared for sampling. The area was rinsed with 1 – 2 mL of bone wash and then cleaned using sterile swabs. The bone was transferred to a weigh boat and allowed to air-dry. Swabbed areas were gently sanded using a Dremel rotary tool, fitted with a 1/4 inch sanding band, until the outer brown surface material was removed and clean cortical bone revealed. A second wash of the sanded area was conducted to remove any residual dust generated during sanding. Finally, the area was rinsed using sterile water and the fragment allowed to air dry. Bone powder was generated for the DNA extraction process by drilling lightly into the sanded area using a Dremel rotary tool fitted with a 1/16 inch drill bit. Twenty-five to 50 mg of bone powder was collected on a piece of weigh paper, transferred to a 1.5 mL sterile microcentrifuge tube, and the final weight recorded.

An alternative method was used for smaller bones and bone fragments (e.g., metacarpals and ribs). Following the initial rinse, the Dremel tool was fitted with a 1/16 inch drill bit and small holes or nicks, approximately a millimeter deep, were made to

remove the brown surface material. The area surrounding the holes was scrubbed using sterile swabs soaked in buffered wash solution. A new sterile drill bit was attached to the Dremel tool and the initial surface holes were deepened to 1 to 2 millimeters. Bone powder was collected and weighed as described above. Five hundred  $\mu\text{L}$  of digestion buffer and 5  $\mu\text{L}$  of proteinase K (20 mg/mL) were added to each tube containing bone powder. A 1.5 mL sterile microcentrifuge tube containing 500  $\mu\text{L}$  of digestion buffer and 5  $\mu\text{L}$  of proteinase K (20 mg/mL) was prepared alongside the samples to serve as a reagent blank. Samples and associated reagent blanks were vortexed and placed in a 55°C incubator for 24 hours.

#### *Extraction of DNA*

DNA was extracted from the bone powder using an organic method. An equal volume of saturated phenol (500  $\mu\text{L}$ ) was added to each sample, followed by vortexing for approximately 15 seconds, and centrifugation at 14,000 rpm for 5 minutes. The aqueous layer was transferred to new sterile 1.5 mL microcentrifuge tubes. An additional phenol extraction step was conducted if the aqueous layer was colored (ranging from light pink to brown). This was required for most vertebrae and rib samples.

An equal volume of chloroform was added to the aqueous layer. Samples were vortexed for approximately 15 seconds and centrifuged at 14,000 rpm for 5 minutes. The resulting aqueous layer was loaded onto Microcon filter devices and pushed through the column by centrifuging the samples at 10,000 X g for 10 minutes (the Microcon protocol calls for 14,000 X g; however, this was lowered to prevent soil/residual powder from

tearing or clogging the column). The filtrate was discarded and 300  $\mu\text{L}$  of sterile TE (10 mM Tris, 1mM EDTA pH 8.0) was pushed through the column by centrifugation for 10 minutes at 12,000 X g. An additional two TE washes were conducted using this method. DNA was eluted off the column using 20  $\mu\text{L}$  of sterile TE buffer. A one in ten dilution of the extracted DNA was made using sterile TE and used in PCR reactions. DNA samples and dilutions were stored at  $-20^{\circ}\text{C}$ .

### *DNA Amplification using Polymerase Chain Reactions*

Nested PCR was carried out for both MTB complex DNA and human mitochondrial DNA. Primer sequences and PCR parameters are outlined in Table 4. The first round of PCR consisted of 20  $\mu\text{L}$  reactions using 19  $\mu\text{L}$  of master mix and 1  $\mu\text{L}$  of bone DNA extract (1:10 dilution of stock extract). A master mix was prepared using 2  $\mu\text{L}$  of Eppendorf Hot Master Taq Buffer, 2  $\mu\text{L}$  of 30  $\mu\text{g}/\mu\text{L}$  bovine serum albumin, 2  $\mu\text{L}$  of 2  $\mu\text{g}/\mu\text{L}$  deoxynucleoside 5'-triphosphates, 0.4  $\mu\text{L}$  of 20  $\mu\text{M}$  forward, 0.4  $\mu\text{L}$  of 20  $\mu\text{M}$  reverse primer and 1U of Hot Master Taq. Reagent blanks, negative and positive controls were conducted with each set of PCR reactions. Four  $\mu\text{L}$  of the PCR products, from initial amplifications, were electrophoresed on a 3% agarose gel. Ethidium bromide staining of the gel was conducted followed by UV visualization.

Semi-nested or nested PCR was conducted on those samples that contained no visible or a faint product. Semi-nested PCR involved the preparation of a master mix, as described above, replacing the bovine serum albumin with sterile water, and using a primer that was internal to either the initial forward or reverse primer. Nested PCR was

conducted for the MTB complex reactions using forward and reverse primers internal to the initial primer pair. One  $\mu\text{L}$  of the amplified template DNA from the first round PCR was added to 19  $\mu\text{L}$  of the second round PCR master mix. PCR parameters used for the second round are also outlined in Table 4. If no band was visualized in the initial PCR agarose gel then 20 to 25 additional amplification cycles were conducted. If a faint product was visualized then 10 to 15 additional cycles were conducted. Following the second round of amplification 4  $\mu\text{L}$  of the nested PCR products were electrophoresed on a 3% agarose gel and visualized with UV light.

Controls were examined for the presence of PCR product to assess the validity of the results. If a product was seen in the reagent blank the number of cycles used in the second round of PCR was lowered. DNA was re-extracted from the bone sample if a product was visible in the reagent blank after using this lower cycle number.



**Table 4: Primer Sequences and Parameters**

PCR conditions and primer sequences used in the amplification of mitochondrial and MTB Complex DNA are outlined. An initial denaturation step of 94 °C for 5 minutes was conducted prior to cycling. This was followed by a final extension step of 72 °C for 7 minutes.

Target	Primers (5' → 3')	Product Size (bp)	Parameters	Cycle No.	
IS6110*	P1 P2	ctcgtccagcgcgcttcgg cctgcgagcgtaggcgtcgg	123	94°C, 30 sec 68°C 1 min 72°C 30 sec	35
	IS3 IS4	ttcggaccaccagcacctaa tcggtgacaaaggccacgta	92	94°C, 30 sec 64°C 1 min 72°C 30 sec	20 – 25
OxyR*	F R	cgcgctgtcagagctgacttt tctgcggaatcagtgtcacc	150	94°C, 20 sec 66°C 30 sec 72°C 30 sec	35
	F2 R	ttgtgactgcatgaggggc tctgcggaatcagtgtcacc	127	94°C, 30 sec 62°C 30 sec 72°C 30 sec	20 – 25
	SNP(R)	acgcactgcacgacggtggccagc			
Mtp40 <sup>±</sup>	F R	ctggtcgaattcgggtggagt atggtctccgacacgttcgac	152	94°C, 30 sec 64°C 1 min 72°C 30 sec	35
	F2 R	gcaaagttgaacgctgaggt atggtctccgacacgttcgac	131	94°C, 30 sec 63°C 1 min 72°C 30 sec	20 – 25
HV1	15989 16207	ccatgcttacaagcaagt acttgcttgaagcatgggg	218	94°C, 30 sec 56°C 1 min 72°C 1 min	35
	16057 16207	aagtattgactcacccatca acttgcttgaagcatgggg	150	94°C, 30 sec 56°C 1 min 72°C 1 min	10 – 20

\* = Mays et al. (2001)      ± = Forward and Reverse from Fletcher et al. (2003);

Nested primers for Mtp40 and OxyR SNP designed in house.

## *Prevention of Contamination during Ancient DNA Analysis*

The Armed Forces DNA Identification Laboratory (AFDIL) has developed a series of protocols to prevent contamination of ancient DNA sources (Edson et al. 2004). These include the use of personal protective equipment, running appropriate controls, laboratory set-up, and tracking of contamination. All of these measures were utilized in this study. During the extraction process and PCR preparation, facemasks, disposable sleeves, and two pairs of latex gloves were always worn. Laboratory equipment was rinsed with 10% bleach, washed with detergent and subjected to UV light. Reagent blanks, negative, and positive controls were run with every experiment. DNA extracted from a control bone that was known to not contain the pathogen (e.g., bones from individuals who died from trauma, fresh skeletal material, etc) was used as an additional control.

Contamination of the bone samples, DNA extracts, and PCR reactions by pathogen control and exogenous human DNA was of great concern. Dilutions of DNA extracted from *M. tuberculosis*, *M. bovis* and *B. abortus* were used as positive controls when screening for the presence of pathogen DNA. All stock bacterial DNA and dilutions were stored in a -20°C freezer located in a separate laboratory from the main extraction laboratory. PCR experiments were set up by aliquoting the master mix and adding bone DNA extract in a CleanSpot PCR hood. The negative control and bone samples were then placed in a thermocycler and held at 4°C. Bacterial DNA was added to the positive PCR reaction in a separate laboratory, placed in the thermocycler away

from other samples, and the thermocycler started. Care was taken to never return to the extraction laboratory or handle bone samples after using bacterial DNA.

#### *Sensitivity Assays of the MTB Complex PCR Primers*

Methods and primers designed for the detection of MTB complex DNA were assayed for their sensitivity using bacterial genomic DNA. Three 1:1000 dilutions of *M. tuberculosis* and *M. bovis* DNA were prepared. The optical density, at 260 nm, was determined using UV spectroscopy. Absorbencies were used to estimate that the *M. tuberculosis* genomic DNA stock had a concentration of 700 ng/ $\mu$ L and *M. bovis* stocks were at 935 ng/ $\mu$ L. The relative molecular weights of a single genomic copy of *M. tuberculosis* and *M. bovis* were calculated using the method outlined in Table 5.

**Table 5: Calculation of *M. tuberculosis* and *M. bovis* Genome Weight**

The total number of base pairs for the bacterial genomes were obtained from the Sanger Institute website ([www.sanger.ac.uk/](http://www.sanger.ac.uk/)). Molecular weight of the genome in Daltons was estimated by multiplying the total number of bases by the average molecular mass of an A/T or G/C base pair (~660 Daltons). This was used to determine the approximate mass of the genome in femtograms (1 femtogram =  $10^{-15}$  grams).

Species	Length of Genome (bp)	Single Base Pair MW (Da)	Genome MW in Daltons	Dalton → gram Conversion	One Genomic Copy (g)
<i>M. tuberculosis</i>	4411532	660	2911611120	1.67E-24	4.86E-15
<i>M. bovis</i>	4345492	660	2868024720	1.67E-24	4.79E-15

It was estimated that a single copy of *M. tuberculosis* or *M. bovis*'s genome equaled 4.86 femtograms (fg) and 4.79 fg respectively. Using these estimates the *M. tuberculosis* stock contained approximately  $1.44 \times 10^8$  genomic copies/ $\mu\text{L}$  and the *M. bovis* stock approximately  $1.95 \times 10^8$  genomic copies/ $\mu\text{L}$ . Serial dilutions of stocks were prepared so that PCR reactions varied the amount of template from 0.1 to 10,000 genomic copies. PCR inhibition was also assayed by spiking bone sample DNA extracts with low copy numbers of *M. tuberculosis* DNA (1 to 100 copies). Nested PCR was then conducted on the samples to see if the bacterial DNA could be preferentially amplified, in the presence of human DNA, and visualized on an agarose gel.

## *Differentiation of M. bovis and M. tuberculosis*

Semi-nested PCR was conducted for the OxyR gene using the master mix protocol outlined above. Primers and PCR parameters used to target this gene are outlined in Table 4. PCR products were electrophoresed on a 4% agarose gel to determine if amplification was successful and provide an estimate of the amount of DNA present.

A SNP assay was designed with the intent of analyzing any samples that produced positive OxyR products. Methods were first optimized using *M. tuberculosis* and *M. bovis* DNA. SNP reactions were prepared by adding 2  $\mu\text{L}$  of shrimp alkaline phosphatase (SAP) and 1  $\mu\text{L}$  of exonuclease I (Exo1) to the Oxy R PCR reactions. Reactions were incubated at 37°C for 60 minutes followed by denaturing of the enzymes at 75°C for 15 minutes. Single base primer extension assays were conducted using a CEQ SNP-Primer Extension Kit (Beckman). SNP premix was prepared that contained DNA polymerase, reaction buffer, ddATP, and ddGTP CEQ dye terminators. Ten  $\mu\text{L}$  SNP reactions were set up using 5.5  $\mu\text{L}$  of SNP premix, 1  $\mu\text{L}$  of either 0.2  $\mu\text{M}$  or 2  $\mu\text{M}$  OxyR SNP Primer (Table 4), 0.5  $\mu\text{L}$  of DNA template and 3  $\mu\text{L}$  of sterile water. Reactions were subjected to 25 cycles of 96°C denaturation for 10 seconds, 55°C annealing for 5 seconds, and 72°C elongation for 30 seconds. One  $\mu\text{L}$  of SAP was added to each reaction followed by a 60-minute incubation at 37°C, to remove unincorporated dye terminators, and a 75°C hold to deactivate the enzyme.

SNP analyses were conducted by adding 0.5 – 1  $\mu\text{L}$  of the SNP product, 0.5  $\mu\text{L}$  of Beckman-80 size standard, and 38.5 – 39  $\mu\text{L}$  of Sample Loading Solution. SNP-21

parameters (capillary temperature 50°C, denature at 90°C for 60 seconds, inject at 2.0 kV for 30 seconds, and separate at 6.0 kV for 21 minutes) were used for data collection. Raw data were analyzed using the Fragment Analysis Program associated with the CEQ 8000.

#### *M. tuberculosis Mtp40 Primer Optimization and Primer Specificity Assays*

Primers to target the Mtp40 gene were designed and optimized by Kristy Bachus. The primers were used in a semi-nested PCR method designed to target *M. tuberculosis*. Experiments were also conducted to determine the specificity of the Mtp40 primers to *M. tuberculosis*. Primer sets were tested on DNA extracted from a variety of sources including: *E. coli*, soil from a Michigan agricultural site (Meyers 2006), soil from Voegtly cemetery, human blood, human saliva, ancient human bone, fresh human bone, *M. tuberculosis*, and *M. bovis*. Only reactions that contained *M. tuberculosis* genomic DNA produced a PCR product of the appropriate size. Specificity assays, such as the one described above, were also conducted on all other MTB complex primer pairs.

#### *Sequencing of Mitochondrial Hypervariable Region 1*

DNA sequencing was conducted on PCR amplicons using the HV1 primers outlined in Table 4. PCR reactions were purified by diluting the reaction in a total volume of 300 µL sterile water. Diluted reactions were loaded onto a Montage PCR

Centrifugal Device and centrifuged at 1000 X g for 15 minutes. PCR products were eluted from the column by resuspending them in their initial volume using sterile water.

Ten  $\mu\text{L}$  sequencing reactions were prepared using 4  $\mu\text{L}$  of CEQ DTCS Quick Start Kit, 1  $\mu\text{L}$  of 20 mM forward or reverse primer, variable volume of DNA template (~6 ng) and sterile water. Reactions were subjected to the following sequencing parameters: denaturation at 96°C for 20 seconds, annealing at 50°C for 20 seconds, and elongation at 60°C for 4 minutes for 30 cycles. Reverse 16207 often produced poor sequencing results. Increasing the annealing temperature for 16207R to 60°C and the extension to 65°C provided more accurate sequencing results (Murray 2005). Sequencing reactions were halted by adding 2.5  $\mu\text{L}$  of a stop solution (1  $\mu\text{L}$  of 3 M NaOAc pH 5.3, 0.5  $\mu\text{L}$  glycogen, 0.2  $\mu\text{L}$  of 500 mM EDTA, and 0.8  $\mu\text{L}$  of sterile water) to each sample.

DNA was precipitated by transferring the sequencing reactions to 1.5 mL sterile microcentrifuge tubes and adding 30  $\mu\text{L}$  of 95 % cold ethanol. The samples were then vortexed and centrifuged at 14,000 rpm for 15 minutes to produce a DNA pellet. The supernatant was carefully removed and 200  $\mu\text{L}$  of cold 70% ethanol was added. Samples were centrifuged for 3 minutes at 14,000 rpm and the supernatant was removed. The 70% ethanol wash was repeated followed by vacuum drying for 15 – 20 minutes.

DNA pellets were resuspended in 40  $\mu\text{L}$  of Sample Loading Solution, vortexed gently, loaded into a 96 well CEQ sample plate, and covered with a drop of mineral oil. Samples were run using the LFR-1 program associated with the CEQ 8000 Genetic Analysis System (capillary temperature 50°C, denature at 90°C for 120 seconds, inject at 2.0 kV for 15 seconds and separate at 4.2 kV for 60 minutes).

Raw data were analyzed using the Beckman CEQ Sequencing Analysis software. Sequences were aligned using BioEdit (Hall 1999) and compared to the reference sequence (Anderson et al.1981). Forward and reverse HV1 sequences were obtained for a long bone (femur, ulna, or radius), a rib or pelvis, and a thoracic vertebra from each burial. Those bone samples that showed polymorphisms from the Anderson et al. (1981) reference sequence at a particular base were noted. DNA sequences obtained from each bone were compared to one another to produce a consensus sequence for that individual. Results were also compared to the HV1 mtDNA sequences of the analyst to rule out contamination. PCR reactions were repeated if any contamination was noted, followed by re-extraction of DNA from the bone if contamination was seen a second time.

#### *Real-Time PCR Primer Design for Tuberculosis, Brucella and Mitochondrial DNA*

DNA sequences of genes specific to the MTB Complex (IS6110, OxyR' and Mtp40) and *Brucella spp.* (IS6501 and Bcsp31) were obtained from the NCBI Website (Sequence Ascension No: IS6110 (X17348), OxyR'(DQ056361), Mtp40 (M57952), IS6501 (M94960) and Bcsp31(M20404)). These were uploaded into Applied Biosystems Primer Express™ software, and primer pairs were selected that would amplify a 58 – 63 bp region of the target gene. Real-time PCR primers for human mitochondrial HV1 were also used. These had been designed previously by Michael Gehring (2004) and amplified a 118 base pair region of HV1. An additional set of HV1 primers (F16190: R16251) that amplified a 61 bp region were also used (Table 6).



**Table 6: Real-Time PCR Primers**

Primers are organized based on their target species and shown with 5' → 3' directionality.

Target	Species	Forward (5' → 3')	Reverse (5' → 3')	Size (bp)
IS6110	MTB Complex	gcttagcgggcgggacaa	gccgacgggtctttaaaa	62
Oxy R	MTB Complex	gcgacgaatcggtttggt	gcaagacgctgtaggactct	63
Mtp40	<i>M. Tuberculosis</i>	cgcgaaatgacaatgca	ggtccggtggcattcgt	65
IS6501	<i>Brucella spp.</i>	cgcgcggtggattgac	agcggtaggccgatagca	58
Bcsp31	<i>Brucella spp.</i>	gcgttgggagcgagctt	ccagtcccatacggaaaaa	59
HV1	Human mtDNA	(F16190) ccatgcttacaagcaagt	(R16251) ggagttgcagttgatgt	61
HV1	Human MtDNA	(F16400) accatcctcctgaaatcaa	(D-Loop) accctgaagtaggaaccaga	118

#### *Optimization of Real-Time Primers*

Real-time PCR primers were optimized according to the SYBR<sup>®</sup> Green PCR Mastermix Protocol (ABI 2005). Twenty-five  $\mu$ L reactions were prepared that contained 12.5  $\mu$ L of the SYBR Green PCR Mastermix (2X), 2.5  $\mu$ L of 500 – 9000 nM forward and reverse primer, 0.5 ng/ $\mu$ L of DNA template, and the final volume adjusted with sterile water. Dilutions of 200  $\mu$ M primer stocks were made so that the final forward or reverse primer concentrations could be adjusted to 50 nM, 300 nM, and 900 nM respectively. Primer optimization was conducted by setting up reactions that contained the combinations of forward and reverse primer concentrations outlined in Table 6. A small set of reactions that contained the improper template for that primer pair were set up to

test primer specificity (e.g., 0.5 ng of human DNA was added to reactions that contained TB specific primers). All reactions were run in duplicate in a 96 well optical plate.

**Table 7: Combination of Concentrations Used for Primer Optimization.**

Primer concentrations are in nanomolar (nM) and are shown as a ratio of forward to reverse primer.

	F (900nM)	F (300nM)	F (50nM)
R (900nM)	900:900	300:900	50:900
R (300nM)	900:300	300:300	50:300
R (50nM)	900:50	300:50	50:50

Real-time PCR reactions were loaded onto an ABI Prism 7000 thermocycler. An initial 50°C hold for 2 minutes was conducted to activate the enzyme Uracil N-Glycosylase. This was followed by a 10-minute 95°C enzyme deactivation step that simultaneously activates the AmpliTaq Gold DNA polymerase. Reactions were subjected to forty cycles of 95°C denaturation for 15 seconds and one-minute annealing/extension steps at 60°C. Thermal cycling was concluded with the generation of a dissociation curve by ramping of the sample from 64°C to 95°C. Results were analyzed using the ABI 7000 Series software. According to the SYBR Green PCR Mastermix protocol the primer combination that produced the lowest Ct value with the smallest standard deviation is optimal, so these concentrations were used in all future real-time reactions.

### *Real-Time PCR on Ancient Bone Samples*

Twenty-five  $\mu\text{L}$  real-time PCR reactions were prepared using the optimal primer concentrations. Two and a half  $\mu\text{L}$  of template from bone DNA extracts were added to each 25  $\mu\text{L}$  reaction. Additional reactions were set up for each bone that contained 2.5  $\mu\text{L}$  of a 1:10 dilution of the initial extract. All reactions were run in duplicate and screened using primers for the six target genes outlined in Table 6. Negative controls, reagent blanks and appropriate positive controls were run alongside each set of reactions to check for contamination and proper amplification.

Real-time analysis was conducted on the ABI 7000 Prism using the same conditions described above with the exception of 50 cycles rather than 40 as this has been found to produce better results with degraded DNA template (Andreasson et al. (2003). Amplification plots and dissociation curves of the bone samples were compared to those of the positive control to assess whether or not the DNA extract contained the appropriate product. Bone samples that showed positive amplification were run on a 4% agarose gel and stained with ethidium bromide.

**Table 8: Summary of Analysis Conducted on Pathology and Questioned Bones**

Summary of tests conducted on each bone sample. TB PCR= IS6110 and OxyR screening. MtDNA PCR = (X = 15989:16207 amplification) and (X\* = 15989:16207 amplification and sequencing). RT = Real-Time PCR; followed by the region targeted.

Burial #	Bone Sample	TB PCR	MtDNA PCR	RT IS6110	RT OxyR	RT Mtp40	RT IS6501	RT Bcsp31	RT HV1
32*	Rib	X	X	X	X	X	X	X	X
	Femur	X	X						
629*	Rib	X	X						
213	Thoracic Vert	X	X*	X	X	X	X	X	X
	Ischium	X	X*						
	Femur	X	X*						
	Ulna	X	X*						
	Metacarpal	X							
319	Thoracic Vert	X	X*	X	X	X	X	X	X
	Rib	X	X*						
	Femur	X	X*						
	Fibula	X	X						
	Ulna	X							
	Metacarpal	X							
3060	Thoracic Vert			X	X	X	X	X	X
5010	Thoracic Vertebrae	X	X*	X	X	X	X	X	X
	Rib	X	X*						
	Femur	X	X*						
	Fibula	X							
	Metacarpal	X							
4015	Thoracic Vertebrae	X	X*	X	X	X	X	X	X
	Rib	X	X*	X	X	X	X	X	X
	Femur	X	X*	X	X	X	X	X	X
	Pelvis	X	X*	X	X	X	X	X	X
	Metacarpal	X							
2722	Thoracic Vertebrae	X	X*	X	X	X	X	X	X
	Rib	X	X*	X	X	X	X	X	X
	Pelvis	X		X	X	X	X	X	X
	Radius	X	X*	X	X	X	X	X	X
	Fibula	X							
	Metacarpal	X							

## RESULTS

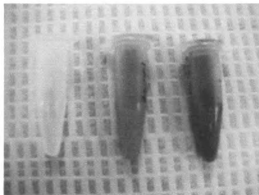
### *Bone Sample Preparation and DNA Extraction*

The bones most often used for analysis were thoracic vertebrae, femora, and ribs. Bones from the pelvis were tested if a burial did not contain a rib, while other long bones (ulna, tibia or fibula) were examined if femora were absent. Drilling of long bones resulted in clean white powder obtained from the cortical bone. In contrast, samples with a high amount of spongy or cancellous material, such as vertebrae and ribs, contained a large amount of dirt and debris. These bones usually resulted in a yellow to brown colored powder.

Following digestion of the bone powder the resulting aqueous layer was clear for long bone samples and red to brown for others (Figure 6). While some of the red or brown color could be removed during the organic extraction it was impossible to remove all of it. This resulted in DNA extracts from vertebrae and rib samples having a light brown or black coloring.

#### **Figure 6: Variability of Aqueous Layers**

Color variation of bone preparations from burial 4015 (image taken following first phenol extraction). On the left is white/light yellow colored extract resulting from the digestion of femur bone powder. The tube in the middle is the typical coloration of a rib extract while the tube on the right is contains digested powder from the vertebral body.



## *MTB Complex Primer Optimization and Sensitivity Assays*

Primer concentrations and annealing temperatures were optimized on *M. tuberculosis* and *M. bovis* DNA. All MTB complex primer pairs gave a clean product using 20  $\mu\text{M}$  of forward and reverse primer except IS6110. The primer pair designed to target IS6110 was optimized at a concentration of 10  $\mu\text{M}$  forward primer to 10  $\mu\text{M}$  reverse primer. Optimum annealing temperatures were determined using a temperature gradient ranging from 55°C to 70°C. All primer pairs had optimum annealing temperatures close to those previously published and are reported in Table 4.

Primer sensitivity assays were conducted using 100,000 to 0.1 copies of the *M. tuberculosis* or *M. bovis* genome as template in PCR reactions. Minimum detection levels for the external primer sets ranged from 10 – 150 genomic copies after 35 cycles of amplification (Table 9). Semi-nested PCR was required for reactions that contained fewer than 100 copies of template to produce a visible product. Following an additional 25 cycles of amplification sensitivity levels ranged from 1 – 15 copies depending on the primer pair. An example of a primer sensitivity assay for IS6110 can be seen in Figure 7.

**Figure 7: Primer Sensitivity of IS6110 on *M. tuberculosis* DNA Dilutions**

Ten  $\mu\text{L}$  PCR reactions were prepared that contained serial dilutions of *M. tuberculosis* template. Following amplification 4  $\mu\text{L}$  of each reaction were loaded onto a 4% agarose gel. (a). PCR using IS6110 forward and reverse primers on *M. tuberculosis* DNA template ranging from 45000 pM to 0.04 pM (~ 100,000 to 0.1 genomic copies). IS6110 PCR products are indicated on the gel by the white arrow. (b). Nested PCR was conducted on the 4.5, 0.45 and 0.045 pM (~10, 1 and 0.1 copies) samples depicted in Figure 7(a). PCR products obtained are outlined in the white box. A 50 base pair ladder is indicated by '50 bp.'

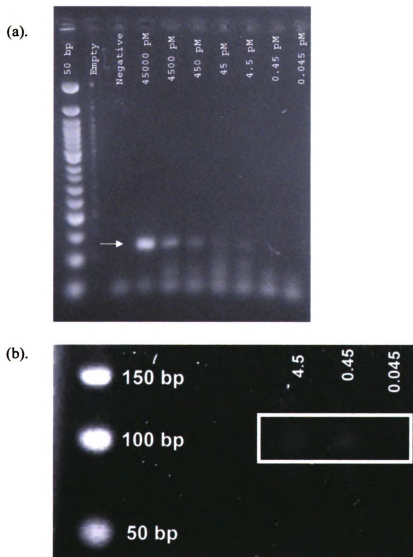


**Table 9: Minimum Number of Genomic Copies Detectable**

Primer sets were tested on 100,000 to 0.1 copies of *M. tuberculosis* (M. TB) and *M. bovis* (M. Bovis) genomic DNA. The lowest number of genomic copies detectable is represented by the value in parentheses. Number under the gene name indicates the number of cycles used. N\_25 = Number of cycles used in nested or semi-nested PCR.

Species	IS6110 (35)	IS6110 (N_25)	OxyR (35)	Oxy R (N_25)	Mtp40 (35)	Mtp40 (N_25)
M. TB	45 fg (~10)	4.5 fg (~ 1)	450 fg (~95)	45 fg (~ 10)	700 fg (~145)	70 fg (~ 15)
M. Bovis	450 fg (~95)	45 fg (~9)	450 fg (~ 95)	45 fg (~10)	N/A	N/A

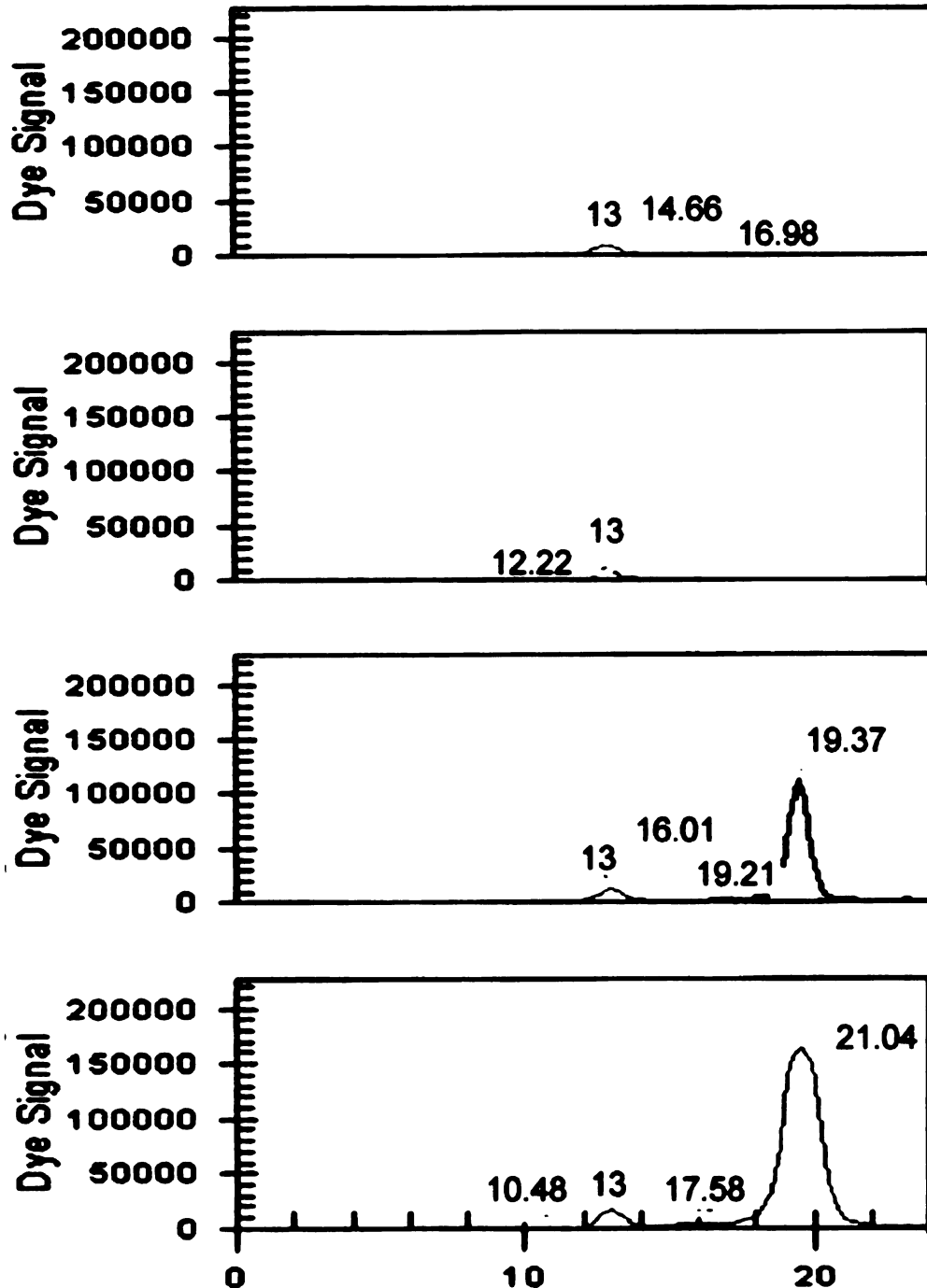
*Optimization of Methods used to Differentiate M. tuberculosis and M. bovis*

Figure 8 depicts results from an OxyR SNP assay optimization experiments. Two sets of SNP extension reactions were prepared; the first used 0.2  $\mu$ M of the OxyR SNP primer and the second used 0.02  $\mu$ M of SNP primer. Reactions were initially conducted with 1  $\mu$ L of PCR product as template. This resulted in a large amount of pull-up and non-target artifact peaks at both primer concentrations. A 1:10 dilution of the initial PCR product was used in future reactions. *M. tuberculosis* produced a black peak at 19.37 corresponding to a cytosine. The *M. bovis* electropherogram shows a blue peak, thymine, at 21.04. DNA base complementarity indicates that *M. tuberculosis* has a guanine at position 285 and *M. bovis* contains an adenine. The negative and human DNA controls did not produce any peaks.



**Figure 8: Differentiation of *M. bovis* from other Members of the MTB Complex**

Results from SNP analysis of base 285 in the OxyR gene. The top two electropherograms correspond to SNP reactions using human DNA and negative control respectively. The third represents results from reactions containing *M. tuberculosis* DNA (black peak at 19.37), while the fourth is from *M. bovis* DNA (blue peak at 21.04). The red peak at 13 is a size standard.

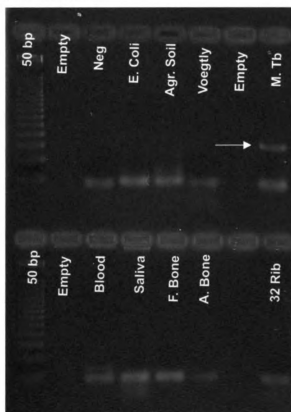


### *Mtp40* Primer Specificity Assays

Only reactions containing *M. tuberculosis* genomic DNA produced a product of the appropriate size for both the external and semi-nested primer pairs (Figure 9). The IS6110 and OxyR primer sets were specific to *M. tuberculosis* and *M. bovis* and did not cross-react with DNA from any other sources. However, when the forward OxyR primer was used with the OxyR SNP primer cross-reactivity with DNA from human saliva was noted.

#### **Figure 9: Mtp40 Specificity**

A one hundred and fifty bp product was only visible in the reaction containing *M. tuberculosis* DNA (indicated by arrow). Bacterial DNA extracted from *E. Coli*, agricultural soil (Agr. Soil), and Voegtly cemetery soil (Voegtly) did not produce any visible product. Human DNA from blood, saliva, fresh bone (F. bone) and ancient bone (A. bone) were also negative. 50 base pair ladder (50 bp), negative control (Neg) and empty lanes (empty) are indicated..

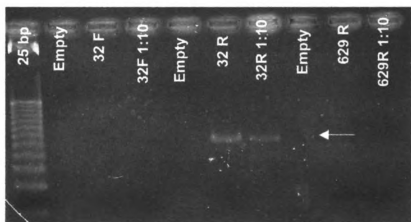


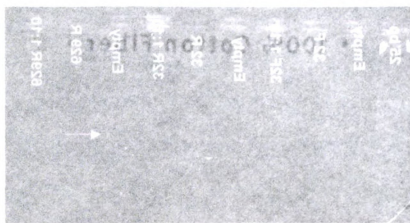
### *Screening of Bone Extracts for Tuberculosis DNA*

DNA was extracted from each Voegtly bone sample three times and PCR screening for the IS6110 element was conducted twice on each extraction. Initial extractions of a femur and rib sample from burial 32 yielded a 123 bp product for IS6110 (Figure 10). DNA was re-extracted from the rib and femur of this burial to determine the reproducibility of results. Only DNA extracted from the rib yielded a reproducible amplicon. Burial 32 extracts did not produce any visible product when used with the OxyR or Mtp40 primer sets. Burial 629 did not produce positive results for any MTB complex assays.

#### **Figure 10: PCR Screening for the Presence of IS6110 in Voegtly Samples**

IS6110 nested PCR on Burials 32 and 629 run alongside a 25 bp ladder (25 bp). Letters indicate the type of bone (F = femur; R =rib) and 1:10 is a tenfold dilution of the neat reaction. Products approximately 123 bp in size can be seen in the 32 rib sample and its dilution (as indicated by arrow). These products correspond to the expected amplicon size for IS6110 (123 bp).





1. The first step is to identify the problem. This involves gathering information about the situation and understanding the underlying causes. It is important to be thorough and objective in this process.

2. Once the problem is identified, the next step is to develop a plan. This involves setting clear goals and determining the best course of action to achieve them. It is important to consider all possible options and to choose the one that is most likely to be successful.

3. The third step is to implement the plan. This involves putting the plan into action and monitoring progress. It is important to stay flexible and to be willing to make adjustments as needed.

4. The final step is to evaluate the results. This involves assessing the effectiveness of the plan and identifying any areas for improvement. It is important to be honest and to take responsibility for the outcome.

Bone samples from Butrint and Diaporit that were screened for IS6110 are outlined in Table 10 and Table 11 along with the number of times DNA was extracted. PCR reactions to screen for IS6110 were conducted a minimum of three times on vertebra, rib/pelvis and a long bone from each individual. Additional bones, such as metatarsals and other long bones, were assayed only in burials that showed signs of pathology. No visible products for IS6110 were obtained from any of the bone extracts. An example of experimental results from vertebrae samples is provided in Figure 11.

**Table 10: Control/Livestock Extracts and IS6110 Experiments**

Number of times each bone sample from the control and livestock groups were drilled (indicated by the 'Number of Extracts'). The number of experiments in which that bone extract was used to screen for the MTB complex is also provided.

Burial Number	Bone Sample	Number of Extracts	Number of Experiments (per extract)	IS6110 Results
<b>10</b>	Thoracic Vertebrae	2	2	Neg
	Left Rib	2	2	Neg
	Fibula	2	2	Neg
	Tibia	1	1	Neg
	Metacarpal	-		Neg
<b>584</b>	Thoracic Vertebrae	2	2	Neg
	Radius	1	1	Neg
	Metatarsal			Neg
	Metacarpal			
<b>M5207</b>	Ulna	1	1	Neg
	Calcaneum	1	1	Neg
<b>M5267</b>	Vertebrae	1	1	Neg
<b>M5509</b>	Ulna	1	1	Neg
	Radius	1	1	Neg

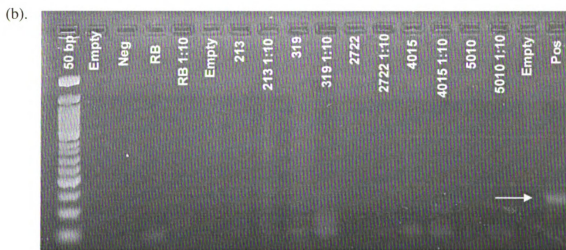
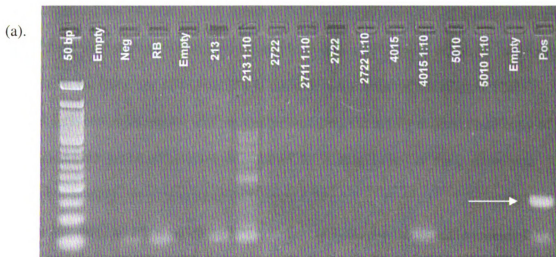
**Table 11: Questioned Pathological Samples and IS6110 Experiments**

The number of time each bone sample from the tuberculosis/brucellosis consistent and questioned pathology groups were drilled (indicated by the 'Number of Extracts'). The number of experiments in which that bone extract was used to screen for the MTB complex is also provided.

Burial Number	Bone Sample	Number of Extracts	Number of Experiments Per extract	IS6110 PCR Results
<b>213</b>	Thoracic Vertebrae	3	3	Neg
	Ischium	2	3	Neg
	Femur	1	3	Neg
	Ulna	1		Neg
<b>319</b>	Thoracic Vertebrae	3	3	Neg
	Rib	2	3	Neg
	Femur	2	3	Neg
<b>5010</b>	Thoracic Vertebrae	3	3	Neg
	Rib	2	3	Neg
	Femur	2	3	Neg
<b>4015*</b>	Thoracic Vertebrae (Body)	6	6	Neg
	Thoracic Vertebrae (Lesions)	2	3	Neg
	Thoracic Vertebrae (Neural Arch)	2	2	Neg
	Rib	3	2	Neg
	Femur	3	3	Neg
	Pelvis	2	2	Neg
	Metacarpal	2	2	Neg
<b>2722*</b>	Thoracic Vertebrae (Body)	8	6	Neg
	Thoracic Vertebrae (Lesions)	3	3	Neg
	Thoracic Vertebrae (Body)	2	2	Neg
	Rib	3	4	Neg
	Pelvis			Neg
	Radius	3	3	Neg
	Fibula	1	1	Neg

### Figure 11: Screening of Vertebrae Samples for IS6110 using Nested PCR

DNA extracted from vertebrae was screened for the IS6110 element. Reactions were conducted as a neat reaction and at 1:10 dilutions. (a) Reactions following 35 cycles using the IS6110 external primers. (50 bp = 50 bp ladder, Empty=no sample loaded, Neg = negative control, RB = reagent blank, and Pos = positive control). Only the positive control produced an amplicon of the appropriate size (arrow). (b) Nested PCR for IS6110 conducted for an additional 30 cycles. Only the positive control produced an amplicon (93 bases) of the appropriate size.

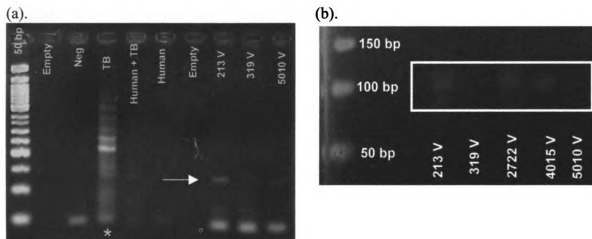


## Spiking Human Bone DNA Extracts with *M. tuberculosis* Genomic DNA

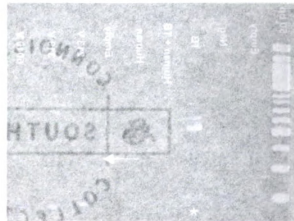
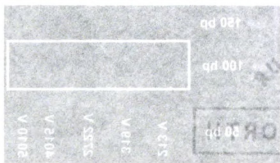
The sensitivity limits of the IS6110 PCR assay, previously determined using bacterial DNA, were tested in the presence of vertebrae DNA extracted from burials 213, 319, 2722, 4015, and 5010. The first experiment consisted of spiking each reaction with ~100 copies of the *M. tuberculosis* genome prior to amplification. Gel electrophoresis of the PCR product indicated that it was possible to detect 100 copies of the *M. tuberculosis* genome, in the presence of human DNA, without using nested PCR (Figure 12a). A second series of experiments was conducted assaying the ability to detect one copy of the *M. tuberculosis* genome using semi-nested PCR. A single copy of the genome was detectable in three out of five samples (Figure 12b).

### Figure 12: IS6110 PCR on Bone DNA Extracts Spiked with *M. tuberculosis* DNA

Figure (a) depicts the detection of 100 copies of *M. tuberculosis* genomic DNA using the PCR method designed to target IS6110 (PCR products are indicated by the white arrow). Figure (b) depicts the IS6110 nested PCR protocols ability to detect concentrations as low as one copy of the *M. tuberculosis* genome (PCR products are outlined by white box) in the presence of human DNA extracted from vertebrae (V). Negative control (Neg), positive control (TB (\* = over amplified)), human control DNA spiked with one copy of *M. tuberculosis* (Human +TB) and human control DNA (Human)) were also conducted in (a).





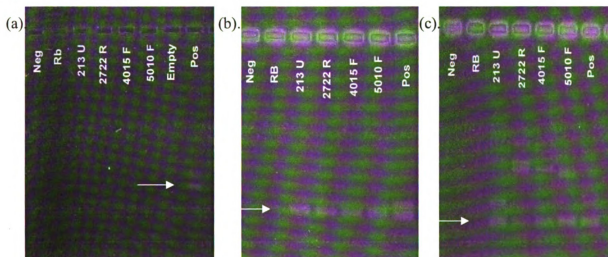


## Mitochondrial DNA Amplification

PCR reactions for mtDNA HV1 were conducted on DNA isolated from vertebrae, ribs/pelvises, and long bones. Initially a neat reaction (1  $\mu$ L of DNA extracted from bone into 19  $\mu$ L master mix) and a 1:20 serial dilution were used. However, after repeated experiments it was found that neat reactions were usually inhibited or did not amplify. Given this, semi-nested PCR needed to be conducted on all extracts in order to obtain a product for sequencing. Long bone samples required fewer cycles during the second round of amplification than vertebra and rib samples. PCR reactions of long bone samples also had a higher tendency to over amplify. Over amplification was corrected by dropping the number of cycles during semi-nested PCR from 20 – 25 to 10 – 15 (Figure 13).

### Figure 13: Semi-Nested HV1 Results using DNA Extracted from Long Bones

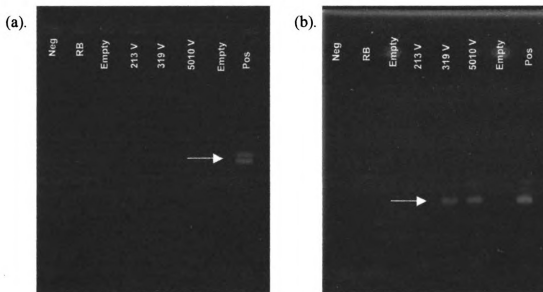
Amplification of 1:10 dilutions of mtDNA extracted from long bones. Numbers correspond to burial number and letter to bone type (U=ulna, R=radius, and F=femur). (a). Results following 35 cycles of amplification. The double band in the positive control is an artifact witnessed with the primer set 15989F:16207R. (b & c). Products obtained after 10 and 20 cycles of semi-nested PCR. Products in (b) are examples of those used for cycle sequencing, while (c) are over amplified. The white arrows indicate PCR products of the appropriate sizes.

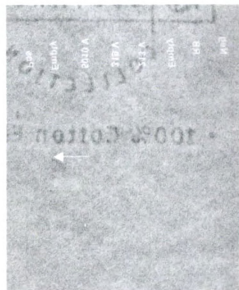
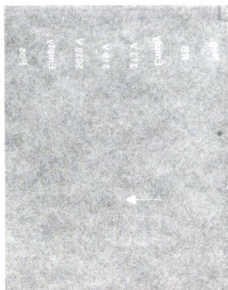


DNA extracted from ribs and vertebrae required a higher number of cycles than long bones. Following the initial 35 cycles an additional 20 to 25 cycles of PCR were conducted. Rib and vertebra DNA extracts, especially samples from burials 213 and 5010, had a high incidence of inhibition. The bones from individual 213 had a red color, which was carried over to the DNA extracts. Similarly, the bones from individual 5010 contained a greater amount of soil than the other burials. Despite additional washes during the sample preparation and selecting areas for drilling that did not contain a large amount of debris, the extracts were black in color. Inhibition of the PCR reactions was overcome by the addition of BSA in the first round and also by diluting the initial DNA extracts at 1:20 rather than 1:10. An example of inhibition can be seen in the lane containing reaction 5010V in Figure 12 (b). This is indicated by the lack of amplification of the product and the absence of primer dimer.

**Figure 14: HV1 Semi-Nested PCR of Vertebrae Extracts**

Example of semi-nested PCR results on a region of HV1 in mitochondrial DNA. Figure (a) shows reactions following 35 cycles of amplification. Figure (b) shows the same samples after nesting the reactions for 25 cycles using internal primer set 16057F:16207. The white arrows indicate PCR products of the appropriate sizes.





### *Hypervariable Region I Sequencing*

Table 12 lists the bone samples used for sequencing and the ranges of HV1 sequences obtained. Forward and reverse sequences from vertebrae, ribs and a long bone were obtained for burials 213, 319, 2722 and 5010. Sequence was not obtainable from burial 4015's vertebra despite successful amplification using semi-nested PCR. Failure appeared to be due to a lack of DNA template in the sequencing reactions or the results could not be analyzed using the CEQ 8000 software.

**Table 12: Ranges of HV1 Sequence Obtained for each Bone**

The range of sequence obtained for HV1 organized by burial number and bone type.

Burial	Bone Sample	Range of HV1 Sequence Obtained	Total Number of Bases
213	Ulna	16059 – 16208	149
	Rib	16082 – 16204	122
	Vertebra	16060 – 16205	145
319	Femur	16069 – 16213	144
	Rib	16081 – 16203	122
	Vertebra	16082 – 16204	122
2722	Femur	16088 – 16216	128
	Rib	16058 – 16203	145
	Vertebra	16058 – 16206	148
4015	Femur	16060 – 16206	146
	Rib	16058 – 16207	149
5010	Femur	16098 – 16204	106
	Rib	16058 – 16203	145
	Vertebra	16058 – 16205	147

The sequencing results from each bone are outlined in **Appendix A: HV1**

**Sequences from Individual Bone Samples.** These sequences were compared to one another and the Anderson et al. (1981) reference to determine a consensus sequence for each individual. A degenerate base was called if two bones from the same individual had a different base at a single site (for example burial 5010 rib and vertebra showed a C at position 16103; while the femur showed a T; therefore the position was called a Y). A comparison of consensus sequences is provided in Table 13. The sequence of the analyst throughout this region is also provided to demonstrate that sequences obtained were not a result of contamination.

**Table 13: Consensus Sequences Derived from Bone Samples for Pathogen Burials**

Consensus sequence for each burial compared to the Anderson et al. (1981) reference sequence. A lack of a letter in a box indicates that the individual contained the same base as the reference at that particular position. Grey boxes denote areas where sequence was not obtained at that site for that particular individual. R = A or G; M= A or C; Y = C or T.

	16059	16077	16078	16094	16103	16112	16193	16199
Anderson	A	A	G	T	T	C	A	T
Analyst		G		C				
Burial #								
213				C				A
319					R			A
2722				C			M	A
4015								
5010	T		A		Y	Y		

### *Real-Time PCR Optimization*

Different combinations of forward and reverse primer concentrations were used to optimize real-time PCR conditions. The concentrations that produced the lowest Ct value and smallest standard deviation between duplicates were selected and used for all further studies. Concentrations, average Ct and standard deviations for the all genes are outlined in Table 14.

**Table 14: Optimum Primer Concentration and Average Ct Values for Primer Pairs**

Primer concentration ratios that gave the lowest Ct and smallest standard deviations are reported for each gene as the concentration of forward to reverse in nM.

Primer Target	Optimum Primer Concentration Forward/Reverse (nM)	Average Ct
IS6110	300:300	16.80
OxyR	900:300	22.40
Mtp40	300:900	19.31
IS6501	900:900	19.02
Bcsp31	900:900	21.11
HV1 (61 bp)	300:300	20.70
HV1 (118 bp)	300:300	19.86



### *Real-Time PCR Results of Voegtly Cemetery Samples*

Real-time PCR reactions were conducted on DNA extracts from Voegtly cemetery's burial 32 that had previously tested positive for IS6110. Amplification of mtDNA (Figure 15) and IS6110 were successful. Dissociation curves of PCR products obtained from bone DNA extracts were compared to those of positive controls. If the curves contained similar overall patterns (i.e. the plots of the positive and questioned samples had a similar shape) and average melting temperatures then the extracted samples and the positive controls were assumed to have amplified the same product. Figure 16 shows the dissociation curve for the mtDNA reactions. Human control DNA and reactions containing burial 32 rib DNA had similar average  $T_m$  (75.4°C and 76.2°C respectively). Figure 17 shows the dissociation curve for the IS6110 PCR reactions. The average  $T_m$  for the *M. tuberculosis* IS6110 product was the same as the product obtained from 32 rib (81.4°C). Amplification seen in the negative controls or reagent blank usually had a lower  $T_m$  and most likely resulted from primer dimer or small artifact products. This indicates that both mtDNA and the IS6110 element were successfully amplified from the burial 32 rib reactions. Results verified that MTB complex DNA was present in the bone extract and indicates the individual had tuberculosis.

**Figure 15: MtDNA Amplification Plot for Voegtly Burial 32 Rib**

Human mtDNA real-time PCR amplification plot. Plot is depicted as Cycle Number vs. Delta Rn (relative fluorescent units). Human DNA positive controls and burial 32 rib (32R) reactions are depicted. 32R #1 is the first reaction and 32F #2 is the duplicate. Red line is a negative control and the green line is the reagent blank from the extraction.

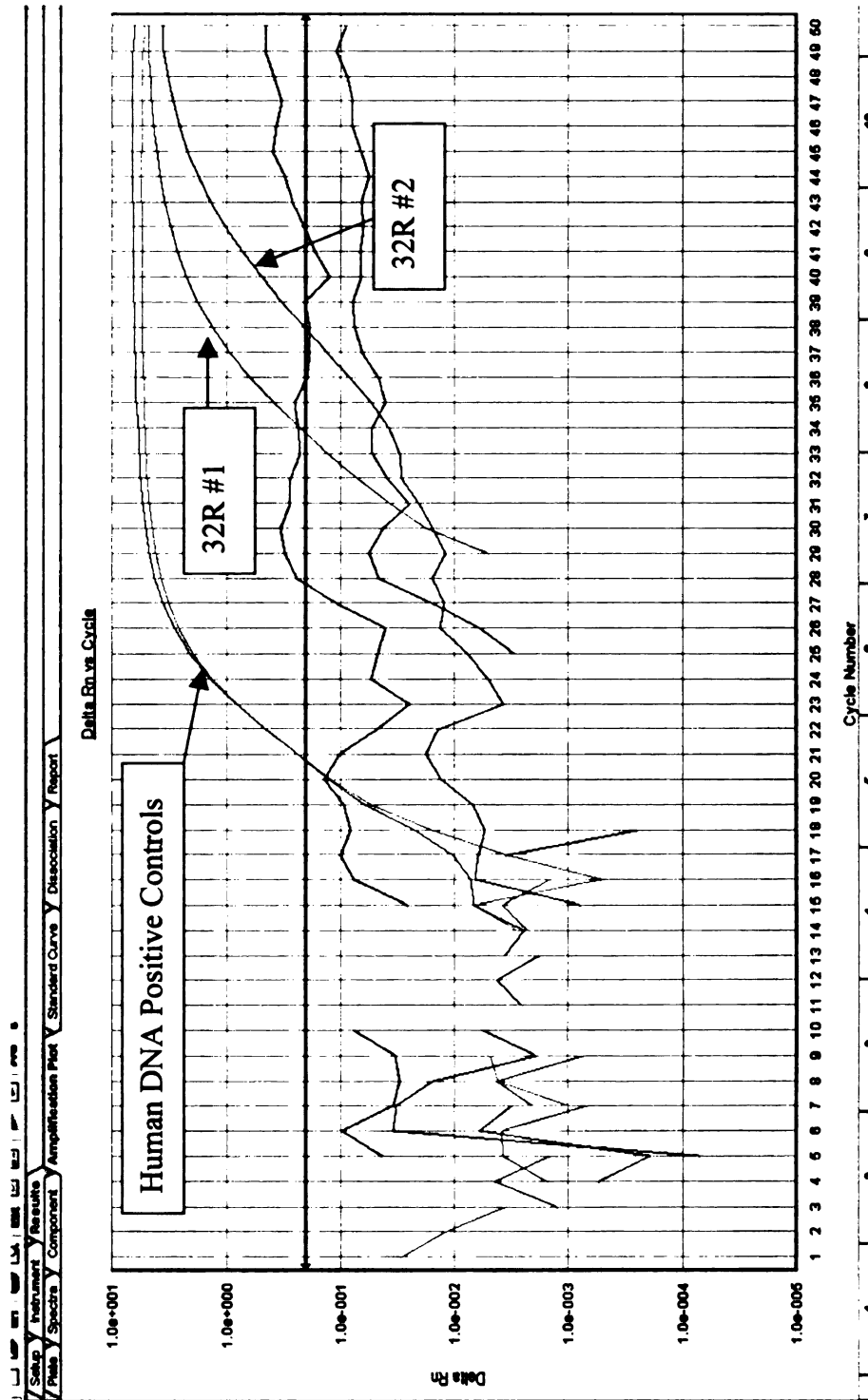


**Figure 16: mtDNA Dissociation Curve for Voegtly Burial 32 Rib**

Dissociation of mtDNA PCR products as a function of Temperature vs. Derivative of the dissociation curve. Positive controls in this image are indicated by the yellow and turquoise line. The blue and purple lines indicate burial 32R PCR reactions. Negative controls and reagent blanks are the green and red lines respectively. The positive controls (human control DNA) had an average  $T_m$  of 76.2°C and reactions containing 32 rib DNA template 75.4°C.

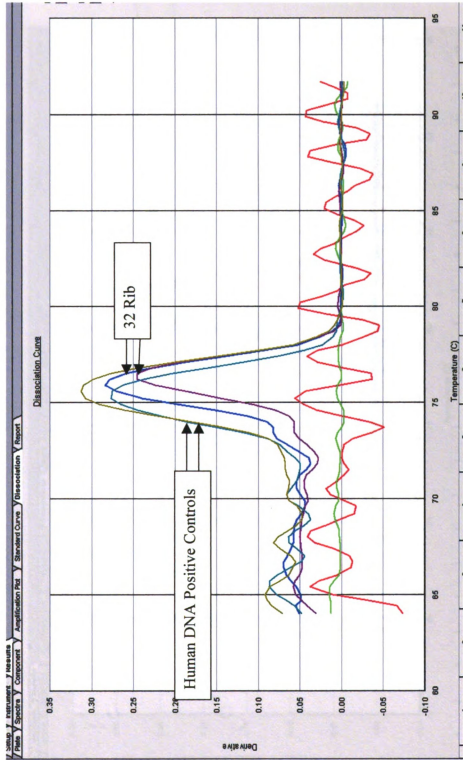


**Figure 17: IS6110 Dissociation Curve for Voegtly Burial 32 Rib**

Dissociation of IS6110 PCR product as a function of Temperature vs. Derivative of the dissociation curve. Positive controls are indicated by the blue and purple line. One of the burial 32 rib DNA (32R) PCR reactions is indicated by the red line; the duplicate reaction did not amplify. The green and purple lines with no signs of amplification represent the negative control and reagent blank. Both positive controls (human control DNA) and one of the reactions containing 32 rib DNA template had an average  $T_m$  of 81.4°C. The duplicate 32R reaction (32R #2) produced a non-specific product with a  $T_m$  lower than the positive control.

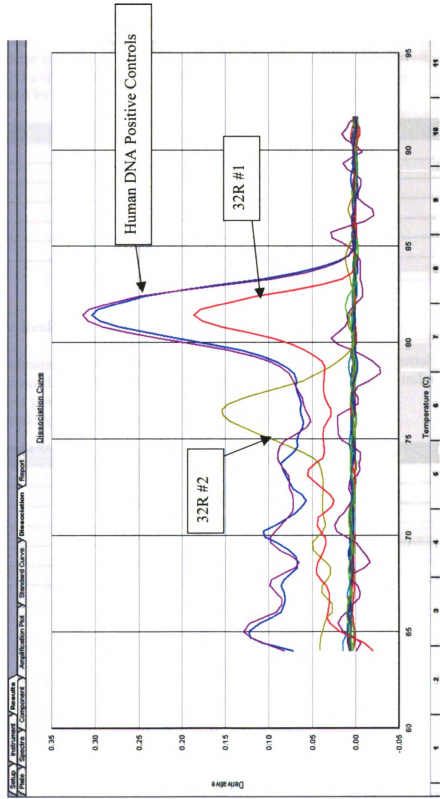


**Table 15: Summary of Real-Time Results for Voegtly Burial 32 Rib mtDNA**

Ct-values and melting temperature (T<sub>m</sub>) data obtained during the amplification of mtDNA extracted from burial 32 rib. HV1 (61 bp) indicates that the smaller 61 bp primer set was used in these experiments. The Ct values refer to the cycle number in which the product crossed a set threshold. Reactions that did have any detectable amplification are indicated by Undetermined. \*=duplicate reaction

PCR Reaction	Ct Value	T <sub>m</sub> (°C)
Negative	Undetermined	71.2
Reagent Blank	Undetermined	69.2
HV1 (61 bp)	33.73	75.9
HV1 (61 bp)*	37.89	76.5
HV1 Positive	20.71	75.2
HV1 Positive*	20.66	75.6

**Table 16: Summary of Real-Time Results for Voegtly Burial 32 Rib IS6110**

Ct-values and T<sub>m</sub> data obtained during the amplification of IS6110 extracted from burial 32 rib. One of the reactions that contained 32 rib DNA produced a product with a similar T<sub>m</sub> as the *M. tuberculosis* positive control. Reactions that did have any detectable amplification are indicated by Undetermined. \* = duplicate reaction

PCR Reaction	Ct Value	T <sub>m</sub> (°C)
Negative	Undetermined	71.5
Reagent Blank	Undetermined	87.8
IS6110	43.32	81.4
IS6110*	Undetermined	82.0
Positive Control	27.52	81.4
Positive Control*	27.05	81.4

### *Real-Time PCR Results for Butrint and Diaporit Pathological Samples*

Real-time PCR experimental results for burial 4015 vertebra are provided in Figures 18 – 21. Mitochondrial DNA and *Brucella spp.* genes (IS6501 and Bcsp31) were successfully amplified. The amplification plot for mtDNA is shown in Figure 18 and the dissociation curve in Figure 19. PCR reactions containing human control DNA and bone DNA extract produced similar average melting temperatures (75.4°C and 76.2°C). The amplification curve and dissociation curve for IS6501 are depicted in Figure 20 and 21. DNA extracts from 4015 vertebra appeared to have amplified the same product as the *B. abortus* control DNA (average T<sub>m</sub> 81.2°C). The negative control of this sample had a lower T<sub>m</sub> of 77.8°C. The IS6501 negative control, positive control, Bcsp31, and IS6501 real-time PCR reactions were electrophoresed on an agarose gel (Figure 22). Results indicated that the product produced in the negative control was different from those in the samples and positive control. Furthermore, the gel confirmed that the PCR products amplified from the bone were the same size as the positive control.

A summary of real-time PCR result can be found in Table 17. Using real-time methods, mtDNA was successfully amplified from burial 319 vertebra, 2722 ribs and 4015 vertebra, ribs and femur. More importantly, the ribs of individual 2722 produced an amplicon for both Bcsp31 and IS6501, while 4015 produced amplicons for both genes from vertebra and rib samples. Results were verified by conducting real-time PCR for *Brucella spp.* on DNA extracts that had been prepared four months earlier, prior to receiving *B. abortus* control DNA in the laboratory. The Ct values for all positive

reactions are outlined in Tables 18 – 20. Results indicate that *Brucella spp.* DNA was present in the remains of individuals 2722 and 4015.

**Figure 18: MtDNA Amplification Plot for 4015 Vertebra**

Human mtDNA real-time PCR amplification plot. Plot is depicted as Cycle Number vs. Delta Rn (relative fluorescent units). Human control DNA and 4015 vertebra reactions are indicated. Only one of the duplicate reactions amplified and is indicated by 4015 vertebra. The negative control also produced a product, however, the dissociation curve (Figure 19) indicates that this is most likely non-specific amplification. The reagent blank is also indicated on the plot.

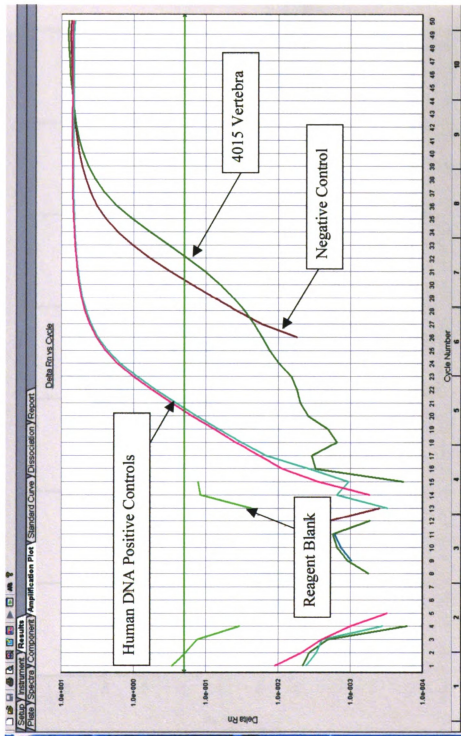




**Figure 19: MtdNA Dissociation Curve for 4015 Vertebra**

Dissociation of mtDNA PCR product as a function of Temperature vs. Derivative of the dissociation curve. Positive controls (human control DNA) and reactions containing 4015 vertebra DNA template (4015 Vert) had a Tm of 64.2°C and 75.4°C respectively. Negative controls did not amplify, while the red line indicates the reagent blank.

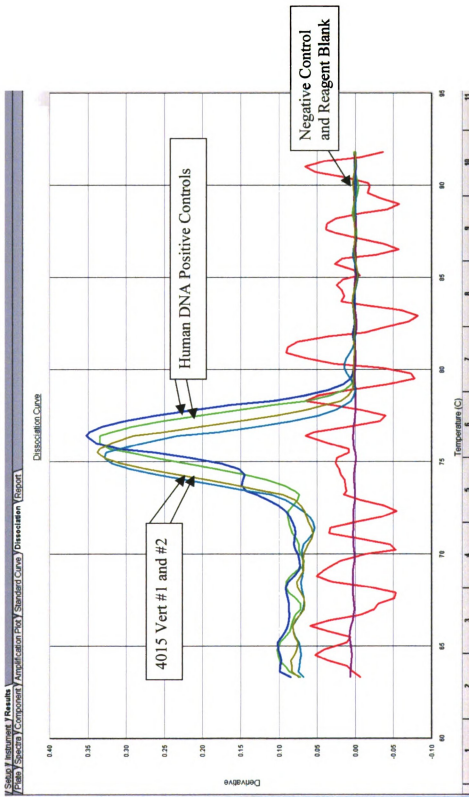


**Figure 20: Real-Time IS6501 Amplification Plot for 4015 Vertebra**

*Brucella spp.* IS6501 real-time PCR amplification plot for burial 4015 vertebra. The plot is depicted as Cycle Number vs. Delta Rn (relative fluorescent units). *B. abortus* control DNA amplification is shown by the light blue and yellow lines while burial 4015 vertebra (4015 Vert#1 and #2) reactions are indicated by the darker green and turquoise line. Amplification was also seen in the negative control reaction as indicated by the black line. No amplification was seen in the reagent blank samples (light green line).

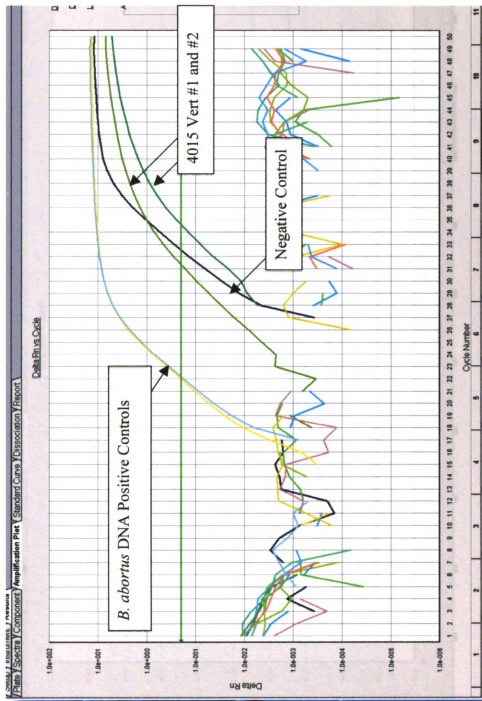


**Figure 21: Real-Time IS6501 Dissociation Curve for 4015 Vertebra**

Dissociation of IS6501 PCR product as a function of temperature vs. derivative of the dissociation curve. Positive controls (*B. abortus* DNA) and reactions containing burial 4015 vertebra DNA template (Vert 4015) had a  $T_m$  of 81.2°C. The negative control also produced a product but with a  $T_m$  of 77.8°C. No product was seen in the reagent blank.

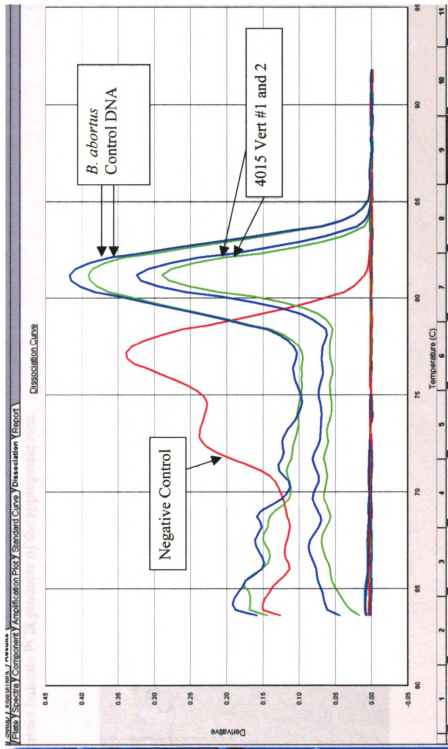


**Figure 22: Agarose Gel of Real-Time PCR Pathogen Results for 4015 Vertbra**

Agarose gels of pathogen DNA products obtained from real-time PCR reactions. A 25 bp ladder was run in each gel, alongside reagent blanks (RB), negative controls (Neg), and positive controls (Pos). Duplicate reactions were run on a gel as indicated by 4015 NA and 4015 NA\* (NA = DNA Extract from the neural arch of vertebral bodies). (a) Real-time PCR reactions that screened for members of the MTB complex using IS6110. No amplification was seen in the bone samples. (b) Real-time PCR reactions that screened for *Brucella spp.* IS6501. (c) Real time PCR reactions that screened for *Brucella spp.* Bcsp31. Note that only one of the duplicates produced a visible product. Results indicate the 4015 vertebra neural arch extract contained DNA from *Brucella spp.* The white arrows indicate PCR products of the appropriate size.

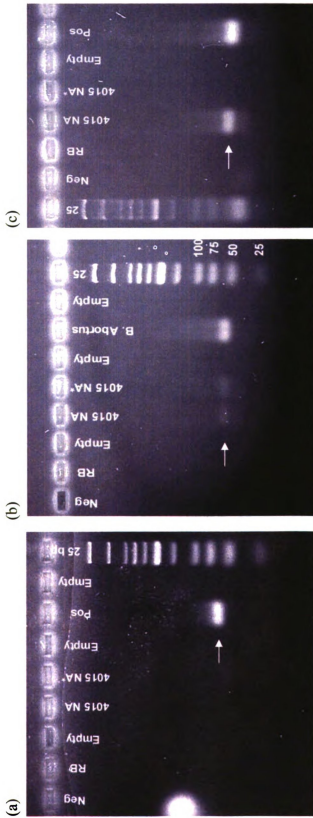


**Table 17: Summary of Real-Time Results**

Bone extracts used in real-time assays. HV1-RT indicates real-time PCR assays for mtDNA HV1 and IS6501-RT/Bcsp31-RT identifies real-time assays for *Brucella spp.* A positive result (Pos) indicates that the sample amplified and the product had a similar T<sub>m</sub> and dissociation curve as the control DNA. All bones were negative in MTB complex real-time assays. \* = Older Extracts Drilled 5/7/06 – 5/20/06 ; all others are from 8/10/06. ± = Extract was very dark in color; additional 1:10 dilution conducted

Burial	Bone/Extract	HV1-RT	IS6501-RT	Bcsp31-RT
219	Vertebra	-	-	-
319	Vertebra	Pos	-	-
5010	Vertebra	-	-	-
2722	Vertebra*	-	-	-
	Vertebra Neural Arch	-	-	-
	Vertebra Body	-	-	-
	Vertebra Lesions	-	-	-
	Rib*	-	Pos	-
	Rib	Pos	Pos	-
	Rib (1:10)±	Pos	Pos	-
	Radius*	-	-	-
4015	Vertebra*	Pos	-	-
	Vertebra Neural Arch	Pos	Pos	Pos
	Vertebra Body	-	-	-
	Vertebra Lesions	-	-	-
	Rib *	Pos	Pos	Pos
	Rib	-	-	-
	Femur*	Pos	-	-

**Table 18 (a – f): Ct Values and Tm for MtDNA Positive Reactions**

Ct-values and Tm data obtained during the amplification of mtDNA from burials 319 vertebra, 2722 rib, 4015 vertebra, 4015 rib and 4015 femur. Lower and higher than average Tm values seen in negative controls and reagent blanks are the result of non-specific amplicons/primer dimers. All DNA extracts were prepared in August of 2006 except those indicated which were prepared four months earlier in May of 2006 (\* = duplicate reactions). Reactions that did have any detectable amplification are indicated by Undetermined.

**(a) Burial 319 Vertebra**

PCR Reaction	Ct Value	Tm (°C)
Negative	Undetermined	70.3
Reagent Blank	Undetermined	69.2
HV1 (61 bp)	33.73	76.5
HV1 (61 bp)*	33.86	76.8
Positive Control	20.71	75.2
Positive Control*	20.66	75.6

**(b) Burial 2722 Rib and 2722 Rib (1:10) Dilution**

PCR Reaction	Ct Value	Tm (°C)
Negative	Undetermined	89.4
Reagent Blank	Undetermined	82.1
HV1 (61 bp)	27.66	74.9
HV1 (61 bp)*	40.5	78.1
HV1 (61 bp) 1:10	31.02	76.4
HV1 (61 bp) 1:10*	31.77	76.4
Positive Control	18.11	75.5
Positive Control*	19	75.8

**(c) Burial 4015 Vertebra\* (May 2006 Extract)**

PCR Reaction	Ct Value	Tm (°C)
Negative	Undetermined	80.4
Reagent Blank	34.00	78.1
HV1 (61 bp)	36.89	76.5
HV1 (61 bp)*	Undetermined	67.6
Positive Control	22.16	74.4
Positive Control*	21.73	76.5

**(d) Burial 4015 Vertebra Neural Arch**

PCR Reaction	Ct Value	T <sub>m</sub> (°C)
Negative	34.12	69.0
Reagent Blank	Undetermined	70.5
HV1 (61 bp)	30.27	76.0
HV1 (61 bp)	32.15	76.4
Positive Control	20.53	75.2
Positive Control*	20.32	75.5

**(e) Burial 4015 Rib\* (May 2006 Extract)**

PCR Reaction	Ct Value	T <sub>m</sub> (°C)
Negative	Undetermined	70.3
Reagent Blank	Undetermined	69.2
HV1 (61 bp)	32.72	76.8
HV1 (61 bp)	34.16	76.8
Positive Control	20.71	75.2
Positive Control*	20.66	75.6

**(f) Burial 4015 Femur**

PCR Reaction	Ct Value	T <sub>m</sub> (°C)
Negative	Undetermined	80.4
Reagent Blank	34.00	78.1
HV1 (61 bp)	35.46	76.5
HV1 (61 bp)	33.95	76.8
Positive Control	22.16	74.4
Positive Control*	21.73	76.5

**Table 19 (a – e): Ct Values and Tm for IS6501 Positive Reactions**

Ct-values and melting temperature (Tm) data obtained during the amplification of IS6501 from burials 2722 rib, 4015 rib, and 4015 vertebra. Lower Tm values were seen in some negative controls and reagent blanks as a result of non-specific amplicons/primer dimers. All DNA extracts were prepared in August of 2006 except those indicated which were prepared in May of 2006 (\* = duplicate reactions). Reactions that did have any detectable amplification are indicated by Undetermined.

**(a) Burial 2722 Rib\* (DNA extracted in May of 2006)**

PCR Reaction	Ct Value	Tm (°C)
Negative	37.76	69.2
Reagent Blank	36.34	69.2
IS6501	34.74	78.7
IS6501*	36.32	79.0
Positive Control	20.19	81.7
Positive Control*	20.24	81.7

**(b) Burial 2722 Rib and Rib (1:10)**

PCR Reaction	Ct Value	Tm (°C)
Negative	Undetermined	66.1
Reagent Blank	Undetermined	66.1
IS6501	31.65	81.5
IS6501*	32.57	81.5
IS6501 (1:10)	30.93	81.2
IS6501* (1:10)	21.17	81.5
Positive Control	18.77	81.8
Positive Control*	18.41	81.5

**(c) Burial 4015 Rib\* (DNA extracted in May of 2006)**

PCR Reaction	Ct Value	Tm (°C)
Negative	37.76	69.2
Reagent Blank	36.34	69.2
IS6501	34.8	79.9
IS6501*	37.03	78.7
Positive Control	20.19	81.7
Positive Control*	20.24	81.7



**(d) Burial 4015 Neural Arch**

<b>PCR Reaction</b>	<b>Ct Value</b>	<b>T<sub>m</sub> (°C)</b>
Negative	35.62	77.2
Reagent Blank	38.2	78.4
IS6501	34.54	81.2
IS6501*	31.31	81.2
Positive Control	22.00	81.2
Positive Control*	22.12	81.2

**(e) Burial 4015 Rib\* (DNA extracted in May of 2006)**

<b>PCR Reaction</b>	<b>Ct Value</b>	<b>T<sub>m</sub> (°C)</b>
Negative	37.76	69.2
Reagent Blank	36.34	69.2
IS6501	34.74	78.7
IS6501*	36.32	79.0
Positive Control	20.19	81.7
Positive Control*	20.24	81.7

**Table 20 (a – b): Ct Values and Tm for Bcsp31 Positive Reactions**

Ct-values and melting temperature (Tm) data obtained during the amplification of Bcsp31 from burial 4015 rib and vertebra. Lower Tm values were seen in some negative controls and reagent blanks as a result of non-specific amplicons/primer dimers. All DNA extracts were prepared in August of 2006 except those indicated which were prepared in May of 2006 (\* = duplicate reactions). Reactions that did have any detectable amplification are indicated by Undetermined.

**(a) Burial 4015 Vertebra Neural Arch**

PCR Reaction	Ct Value	Tm (°C)
Negative	35.62	78.4
Reagent Blank	38.20	78.4
Bcsp31	34.52	81.5
Bcsp31*	Undetermined	66.3
Positive Control	19.90	81.8
Positive Control*	18.84	80.6

**(b) Burial 4015 Rib (DNA extracted in May of 2006)**

PCR Reaction	Ct Value	Tm (°C)
Negative	32.57	75.6
Reagent Blank	33.08	75.6
Bcsp31	31.45	81.1
Bcsp31*	31.84	76.8
Positive Control	24.06	81.1
Positive Control*	22.39	81.4

## DISCUSSION

Previous research conducted in our laboratory has shown how the analysis of mtDNA from ancient skeletal remains can provide information that would otherwise be unobtainable. Clemmer (2005), Rennick (2005) and Murray's (2006) molecular studies on remains from a tumulus located at Kamenica, in present day Albania, allowed for a better understanding of relatedness, burial patterns, migration, and overall genetic diversity of the region. The research presented here demonstrates an additional way in which DNA analysis can provide information about an individual and their society.

Diseases have been an intricate part of human history since ancient times. Understanding the interaction between ancient people and pathogens is not only of cultural interest, but may also shed light on how human response to epidemics has evolved over time. The analysis of diseases in a culture is traditionally accomplished through the visual examination of remains. Anthropologists include descriptions of pathologies in biological profiles when examining both ancient and modern skeletons. Skeletal pathologies provide insight into the lives of an individual (such as diet, health, medical practices, and possible cause of death) and in a modern forensic science context can aid in human identification based on comparative medical history. Paleopathologists examine the distribution of these lesions in skeletal populations to better understand how epidemics may have affected the society as a whole. The knowledge gained from osteological analysis is limited because skeletal lesions produced by two different disease processes can share striking similarities. As a result, educated guesses on the organisms that could be responsible are made without ever identifying the exact causative agent.

Relying on diagnostic skeletal lesions alone may lead to the misidentification of a disease process, an inaccurate description of the skeletal remains, or a gross underestimate of an endemic pathogen. Ancient pathogen DNA analysis can be used to verify skeletal lesions or abnormalities as originating from a specific organism. This can aid in the development of criteria for the identification of pathogens in skeletal material and provide a better understanding of bone tissues response to infection. Furthermore, the combination of traditional osteological methods and pathogen DNA analysis provides a powerful tool to identify the specific organism infecting an individual and provide a better understanding of the disease's distribution throughout a culture.

#### *Bone Preparation for DNA Extraction*

In this study, the preparation of bone samples varied greatly based on bone type, size, and condition. Bones with a high percentage of cortical material, such as long bones, were the easiest to process as they contained a small amount of soil that could be removed by rigorous cleaning. In contrast, bones with a higher percentage of cancellous material, such as vertebrae, were the most difficult to process. The woven nature of the bone provided a porous structure that trapped dirt and debris. Several different methods were attempted to effectively clean cancellous bone. Swabbing the surface proved difficult because small pieces of cotton became caught on the material. Scrapping of the bone with a sterile spatula only resulted in breakage. An alternative method was tried in which the dirt was flushed out of the crevices. One milliliter of digestion buffer was initially used for this process, but led to the direct disintegration of a large portion of the

bone. Using a wash with a lower concentration of EDTA (10 mM instead of 50 mM) prevented digestion during this step. EDTA is a chelating agent that binds divalent cations, such as the calcium found in bone, and previous studies have shown this chemical's ability to decalcify and break down a bone sample (Sarsfield 2000). The poor quality of the cancellous bone matrix may have allowed it to be completely degraded by the digestion buffer. Flushing of the bone with the alternate wash, followed by gentle swabbing, proved to be the most effective method for cleaning this material prior to drilling.

Drilling cancellous bone also proved to be more difficult than cortical bones. Many more holes were required to generate the 25 – 50 mg of powder necessary for DNA extraction. Sections of cancellous bone also had a higher tendency to break when drilled. Reducing the speed of the Dremel tool and holding the drill bit steady, while stabilizing the bone with forceps, prevented excess fragmentation. Small and brittle bones also had to be handled differently. For example, rib material fragmented or broke in half when drilled at a ninety-degree angle. In this case it was found that holding the drill almost parallel to the bone, while dragging the bit along the surface of the bone, prevented excess destruction of the material. Other samples, such as those from the Voegtly cemetery, were impossible to drill. In these instances the bone surface was washed extensively, small pieces of bone were broken off with forceps and crushed in digestion buffer.

## *DNA Extraction and PCR*

Extraction of DNA from digested bone powder often required the removal of water-soluble components that produced a reddish brown or black color. Performing additional phenol extractions removed a portion of the coloration, yet also led to the loss of some of the DNA template. Pushing the sample through a Microcon also reduced pigmentation of the extract. However, the aqueous layer sometimes left a small amount of residual debris on the column membrane. This debris would clog or tear the membrane if the samples were centrifuged at the maximum speed allowed. Lowering the speed of centrifugation, from 14,000 X g to 10,000 X g prevented damage to the Microcon as well as loss of the DNA samples in the filtrate. A maximum of two additional phenol extractions and three TE washes on the Microcon column removed the highest amount of coloration from the sample without sacrificing DNA template yield.

PCR inhibition was seen with many of the DNA extracts that retained coloration. O'Rourke et al. (2000) found that a large amount of soil-derived PCR inhibitors co-extract with DNA, including tannins, humic acids, and fulvic acids. These inhibitors usually bind directly to Taq polymerase, lowering the success of, or preventing, the amplification of the template DNA. Wilson (1997) reported that diluting or purifying DNA extracts and the addition of a compound with a greater affinity for the inhibitor than the polymerase are the most effective methods to overcome inhibition. The utility of these three methods was demonstrated in this and previous studies (Halvorson 2005, Rennick 2005, Murray 2006). All burials in this study required at least a 1:10 dilution of the DNA extracts in order to amplify successfully. Some extracts (2722 vertebra, 5010

2001

2

001



vertebra, and 213 ischium) retained a dark brown to black color and needed to be diluted 1:20. Diluting DNA extracts, while lowering the amount of starting template, simultaneously decreases the amount of inhibitors present. If inhibition can be overcome while retaining enough starting DNA, then PCR can still be successful. BSA, which is believed to compete with Taq DNA polymerase for the binding of inhibitors, was also added to each reaction. Finally, DNA was concentrated and purified by the use of Microcon spin columns and TE washes. Successful amplification of ancient DNA using these methods demonstrated their ability to reduce PCR inhibition associated with skeletal material.

#### *Contamination and Ancient DNA Analysis*

Ancient DNA analysis requires a high level of sterility to prevent contamination by modern DNA. Contamination can lead to erroneous results, complicate future molecular work, and potentially impair DNA analysis from valuable skeletal material. Wearing personal protective equipment, sterilizing supplies, working under a UV sterilized hood, using different labs for extraction and amplification, and separating positive control DNAs from samples, were all used to prevent contamination in this study. Despite these stringent methods, positive reagent blanks and negative controls for mtDNA were obtained in some experiments.

Contamination usually originated from the analyst or one of the bone samples. If the analyst's sequence was obtained then new PCR reagents were used and the experiment was repeated. PCR reactions were also repeated if the reagent blank or



negative control contained the same sequence as one of the bone samples. In this case DNA was re-extracted from the bone to access the validity of the sequences and ensure that they did not arise from exogenous DNA. Determining the source of contamination not only allowed for the development of methods to prevent it in future experiments but also served as a means of quality control.

Pathogen DNA screening experiments required a few extra precautions. Taylor et al. (1999) recommended that stringent measures be taken including using separate laboratories for DNA extraction and PCR that had not previously been used for microbiology or pathogen DNA work. In this study, IS6110, OxyR, and Mtp40 primer optimization and sensitivity assays were conducted in a separate laboratory from bone experiments. Initially these experiments were conducted using a relatively high concentration of bacterial DNA directly from the stock solution. This led to contamination of all reactions following nested PCR. Contamination probably resulted from the analyst handling the reactions, pipetting, or aerosol (particles of liquid, which may contain minute concentrations of DNA, that are passed through the air from pipetting, opening tubes, etc.). Using a 1:1000 dilution of the bacterial stock as the highest concentration reduced incidences of contamination. Additional safeguards were also implemented such as changing gloves when switching labs, storing stock genomic bacterial DNA in a separate box from dilutions, and ensuring that reactions with the highest concentration of DNA were handled last.

Contamination seen in the optimization experiments also set forth policies in the handling of bone samples. The majority of optimization experiments were completed before the Albanian bone samples were received in the laboratory. In addition, bone

200

2

201



screening and bacterial DNA experiments were never conducted on the same day. Taking these precautions ensured that bacterial DNA samples and questioned bone samples were kept isolated from one another during the entire screening process. Taylor et al. (1999) suggested that positive controls should be used sparingly (i.e. not utilized in every PCR experiment) when conducting ancient DNA analysis. A problem arises that without using positive controls the validity of the results become questionable. An alternative method utilized by Zink et al. (2005) was the use of a positive bone sample rather than bacterial DNA. This was attempted here with the Voegtly material but the irreproducibility of amplification was problematic. Therefore, a better method for future ancient pathogen DNA studies would be to use very low concentrations of bacterial DNA as positive controls, while practicing methods that prevent and monitor levels of contamination.

#### *Human mtDNA Analysis to Assess the Quality of DNA in Skeletal Remains*

Previous studies have shown that human mtDNA can be extracted and amplified from degraded biological sources including skeletal remains, fingernails, and hairs (O'Rourke et al. 2000). Foran (2006) compared the relative degradation of nuclear DNA and mtDNA over time. His results indicated that DNA preservation could be affected by multiple factors, including copy number, chromatin structure, cellular location, and transcriptional activity. MtDNA is retrievable from degraded biological sources because it has a high copy number and may be protected by both the cellular and mitochondrial membrane. Successful extraction and amplification of mtDNA provides evidence that

201

2

201



pathogen DNA, if present, has the potential to be recovered and amplified from the skeletal material.

MtDNA was isolated from vertebra, rib, and long bone samples from each skeleton. Edson et al. (2004) reported that bone type directly influences the success rate of mtDNA extraction, amplification, and sequencing. The authors reviewed casework conducted by AFDIL. PCR of DNA template extracted from long bones had a success rate (measured by the ability to amplify and sequence the control region) of 94.79%, while rib DNA had a rate of 96.15% and vertebrae DNA a rate of 85.71%. Similar results were found in this study with template from long bones requiring fewer PCR cycles to amplify and producing cleaner sequence than DNA from ribs and vertebrae. This indicates that either the femur samples were less physically degraded, had a higher copy number of preserved DNA template, or had less PCR inhibition.

The rib DNA amplification success rate was much lower in this study than those reported by the AFDIL. There are several possible reasons for this discrepancy. First, the Albanian samples tested were much older (the 13<sup>th</sup> century is the latest time period) than those typically studied by the AFDIL (World War II to present). Also, ribs tend to be very fragile and degrade more rapidly than long bones. Second, the AFDIL examines remains from all over the world while the Albanian samples were located in a relatively closed environment. Weather, temperature, soil conditions, bacteria, and moisture could all have affected DNA quality and quantity. Finally, the sample size of the AFDIL study is immensely larger than that of the Albanian bones (1021 vs. 17). The analysis of more long bones, ribs, or vertebrae from Albania could reveal that these bones have similar success rates as those reported by the AFDIL. However, previous research conducted in

200

2

001



our laboratory on Albanian skeletal material has shown success rates that were lower than those produced by AFDIL (Rennick 2005, Murray 2006). Differences in rates are therefore most likely caused by variation in the condition and age of the material.

PCR reactions for mtDNA HV1 were conducted until an amplicon that could be sequenced was attained from a long bone, vertebra, and rib. Sequences were obtained from these bones for all burials with the exception of the vertebra from burial 4015. This bone contained a large amount of irremovable debris and soil. MtDNA PCR products obtained from this sample occasionally appeared smeared or light on an agarose gel. The DNA in the vertebra may have been degraded or extracts may have contained a high concentration of inhibitors. The presence of inhibitors is supported by the fact that extracts from this sample were black in color. Furthermore, a dilution of the DNA extract did allow for amplification but sequencing reactions still failed. In general, bone DNA extracts that were light brown, red, or clear amplified successfully using a 1:10 dilution. In instances where the extracts were dark brown or black the sample had to be diluted further (in this study a 1:20 or higher dilution was required). Darker reactions seemed to contain a higher concentration of inhibitors, which needed to be lowered for the Taq polymerase to work efficiently.

Following successful amplification, HV1 sequences obtained from the vertebra, rib, and long bone were aligned and their polymorphisms compared. The analysis of human DNA when conducting pathogen-screening studies is essential. Successful amplification of mtDNA is a good indicator that, if present, the pathogen DNA should be detectable, as both the human and pathogen DNA were subjected to the same environmental conditions over a similar period of time. In addition, human mtDNA is

expected to be in the remains, unlike pathogen DNA whose presence is uncertain.

Human mtDNA amplification serves as a means to assess whether or not the samples are inhibited or if the DNA has completely degraded. Sequencing of mtDNA products ensures that the amplicon obtained originated from the skeletal material and helps rule out contamination by exogenous DNA.

### *Screening for Tuberculosis in Voegtly Cemetery Material using IS6110*

The screening of DNA extracts for the IS6110 insertion element provided an effective way to detect members of the MTB complex. Methods developed in this study were first tested on Voegtly cemetery burials 32 and 629. Ubelaker et al. (2003) reported success at identifying MTB complex DNA in bone samples from both of these individuals. Only DNA extracts from burial 32 gave a positive product while those of 629 did not produce an amplicon after several attempts. Initially, DNA extracted from the Voegtly material was to be used as a positive control for the screening of ancient material. Irreproducibility of results made the use of these bones as positive controls impossible.

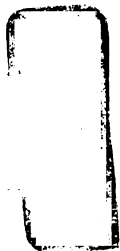
Ubelaker et al. (2003) had similar difficulties and only obtained consistent amplification following whole genome amplification (primer extension pre-amplification (PEP)) of the skeletal DNA extract. In this method PCR reactions are conducted with random oligonucleotide primers to amplify all DNA present in a sample, prior to conducting reactions that target a specific region. PEP was not utilized in this study because previous work has shown low success rates of whole genome amplification on



250

2

001



DNA from Albanian skeletal material (Barber and Foran 2006). PEP is not species-specific and amplifies all DNA present in the reaction. This method could be beneficial when the amount of pathogen DNA template is at a low concentration (i.e. acute infections or highly degraded material), however PEP will also increase even minute amounts of exogenous DNA or contamination in the extract. The risk of contamination leading to erroneous results is therefore magnified when PEP is utilized. Care should be taken when employing this method in molecular pathogen screening experiments because the validity of results is highly questionable.

*Screening for Tuberculosis in the Voegtly Cemetery Material using OxyR and Mtp40*

Burial 32 rib DNA extracts were also screened for the presence of the OxyR and Mtp40 genes. Despite repeated attempts, all PCR reactions containing 32 rib template were negative. Mays et al. (2001 and 2002) had similar results in their molecular assays of medieval remains from the Wharram Percy collection. In the initial study, DNA was extracted from the inside of lesions located on bones (mostly vertebrae) of nine individuals. Seven of these tested positive for IS6110 and Mtp40, while only 6 tested positive for OxyR. Rib DNA from each of these individuals was also screened, resulting in one testing positive for IS6110 and none for the OxyR gene.

Amplification of IS6110 may have been more successful because the genomes of the MTB complex members contain 5 – 20 copies of this insertion element and only single copies of the OxyR and Mtp40 genes. PCR assays that utilized primer sets for the IS6110 element were able to detect a lower copy number of the bacterial genome than

those designed for Mtp40 and OxyR (detection level of 1 vs.100 copies). Mays et al. (2002) also found that assays for IS6110 were more sensitive than those designed to target OxyR or Mtp40 sets (3 vs. 300 copies). The higher copy number of the IS6110 insertion element appears to directly affect the sensitivity and ability to detect the pathogen DNA. Future molecular work on analyzing pathogen DNA from ancient remains would benefit from designing PCR assays that target regions of the genome that are multi-copy.

The inability to amplify the OxyR and Mtp40 genes from the IS6110 positive Voegtly material prevented the identification of which species of the MTB complex material was present. However, the methods developed here may aid in the differentiation of *M. tuberculosis* and *M. bovis* in future studies of ancient remains. The SNP present in the OxyR gene is used to classify a member of the MTB complex as *M. bovis* (Baker 2004). Traditionally, sections of the gene are amplified and sequenced in order to determine what base is present at the species-specific polymorphic site (Baker 2004). Sequencing of this gene has also been used in studies of ancient skeletal material (Donoghue 1998, Mays et al. 2001, Mays et al. 2002). DNA sequencing requires that a rather large (150 – 200 bp minimum) piece of DNA be extracted and amplified from the samples. Obtaining and successfully sequencing this size fragment of DNA could be difficult in highly degraded remains. Single nucleotide extension assays are more effective because the size of the amplicon is smaller (often 40 – 60 bp), the assay is very rapid, and base determination of a single site can be conducted without scrutinizing a large amount of sequence. SNP assays can also be multiplexed so a number of species-

specific polymorphic sites are assayed and a profile for the identification of a particular organism produced.

A semi-nested Mtp40 PCR method was also developed in this study. Previous researchers (Mays et al. 2001, Fletcher et al. 2003) used primer sets that produced a relatively small amplicon (152 bases) and attempted to increase detection limits by using 43 cycles of PCR rather than 35. Mays et al. (2001) reported a minimum detection level of 300 copies using this approach. Primers developed by Mays et al. (2001) were used as the external set for a semi-nested assay designed here. Semi-nested PCR assays improved the sensitivity allowing for the detection of 15 copies. Based on these results semi-nested PCR of the Mtp40 gene may allow for the identification of *M. tuberculosis* in ancient material with a higher efficiency. Further testing would need to be conducted since the Voegtly bone still failed to yield a product for Mtp40 using this method.

#### *Screening for Tuberculosis in Butrint and Diaporit Skeletal Material*

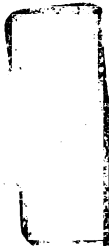
Several sets of skeletal remains from Butrint and Diaporit contained lesions. Similar vertebral and rib lesions were identified on two sets of remains located at the Butrint sites 2722 and 4015. Burial 2722 was from the 11<sup>th</sup> – 13<sup>th</sup> century AD and contained the skeletal remains of an adolescent male. This burial was excavated from the Baptistery and the bones showed multiple lesions on the vertebrae and ribs. The second set of skeletal remains, burial 4015, was excavated from the Merchant's house, and contained an adolescent male from the 11<sup>th</sup> – 13<sup>th</sup> century. One other burial from the Butrint site, 5010, and two others from Diaporit, 213 and 319, showed pathologies that

■

250

2

001



were not entirely consistent with 2722 and 4015. While these burials had porosity of the ribs, long bones, and vertebrae they also contained distinctive skeletal lesions. Examples of distinctive pathologies on these remains include lesions on the parietals of the skull (319 and 5010) and bony projections/growths on the vertebrae (213). These pathologies were not consistent among the five pathological skeletons (213, 319, 2722, 4015 and 5010) utilized in this study. However, Fenton (2006) hypothesized that tuberculosis or brucellosis could still produce these types of lesions and abnormalities based on gross analyses of the remains and comparison to previous studies.

The vertebral and rib lesions seen on the Albanian remains were consistent with the lesions described by Mays et al. (2001 and 2002) in their study of the Wharrum Percy collection. The causative agent behind these lesions was determined to be *M. tuberculosis*. This led to the assumption that tuberculosis was also the causative agent behind the lesions noted on the Butrint and Diaporit bones. However, none of the Albanian bones screened gave a positive result for the MTB complex DNA after a total of 330 assays.

Negative PCR results for pathogen screening assays are difficult to interpret because they can indicate either that the person was never infected or that the pathogen DNA was present but is no longer detectable. Additional experiments were used to assess whether or not the bones were negative for the pathogen. MtDNA analysis confirmed that DNA was preserved in the Albanian bone samples. Primer sensitivity and spiking assays showed that one copy of the tuberculosis genome could be identified, even with a large background of human DNA. Based on these experiments, even if only one copy of the *M. tuberculosis* or *M. bovis* genome remained in the Albanian bones then it

1951

1

107



should have been detected. Experiments such as these allow the analyst to claim that the individuals tested were negative for infection with more confidence.

### *Assessing Bones for Pathogen DNA using Real-Time PCR*

Following the negative results obtained using traditional PCR; the decision was made to try real-time PCR methodologies. In traditional PCR, amplified product is electrophoresed on an agarose gel and visualized by staining. If the concentration of the resulting amplicon is too low, no band will be seen and the results will be interpreted as negative. The real-time system allows the amount of PCR product to be monitored after each cycle. This is beneficial because even a minute amount of amplification can be detected. In addition, highly degraded DNA template can be amplified because the products produced are generally very small (~60 bp). Real-time PCR seems to be a better platform for screening for pathogen DNA because it can address the issues of low copy number and degradation.

Real-time PCR of human mtDNA was conducted on bone samples to once again assess preservation, inhibition, and to determine PCR conditions for reactions containing bone DNA extract (i.e. how much template should be added, the ideal final volume of reactions, etc). Real-time PCR amplification of human mtDNA was first conducted using primers designed by Gehring (2004). Amplification was not seen using this primer pair, perhaps because the targeted region was too large (118 bp) for the degraded template. The decision was made to use a set of primers that target a smaller region of HV1 (61bp), and successful amplification was obtained for 8 out of 19 bone extracts (Voegtly 32 rib;



22

2

20



Albanian 319 vertebrae, 2722 rib, 4015 vertebrae, rib, and femur). These numbers are lower than expected when compared to nested PCR results.

One explanation for this is that the mtDNA primers were not designed using Primer Express software. This software is manufactured by Applied Biosystems to design optimal primer sets for use on the ABI Real-time PCR Systems. As a result, the melting temperatures ( $T_m$ ) of the amplicons were lower than what is traditionally ideal for real-time assays ( $\sim 70^\circ\text{C}$  vs.  $\sim 80^\circ\text{C}$ ). This made it difficult to differentiate between the actual mtDNA product and non-specific products/primer dimers on the dissociation curve. An additional problem could have been that the designed primers targeted regions within HV1. Primer sets for HV1 are typically designed to target conserved stretches of DNA, because people tend to have a high level of variation outside of these regions. It is possible that the mtDNA primers used in the real-time assay targeted a variable rather than conserved region. If an individual's DNA contained polymorphisms at the primer-binding site then amplification would not occur. A better method would be to target a gene whose sequence is conserved among all humans' mtDNA genome (e.g., cytochrome B). These would allow the assessment of mtDNA preservation and amplification with greater efficiency.

To target the causative agents of brucellosis and tuberculosis additional real-time PCR reactions were performed. Real-time assays that screened for the MTB complex were designed to target IS6110, OxyR and Mtp40 genes. Only Voegtly burial 32 rib gave positive amplification of IS6110; all Albanian samples tested negative. The Voegtly material produced a similar dissociation curve and  $T_m$  as the tuberculosis positive control DNA. These results confirmed the findings that individual 32 was

positive for IS6110, previously published by Ubelaker et al. (2003) and presented in this study. They also demonstrate real-time PCR's capability of detecting pathogen DNA and identifying tuberculosis infection. More importantly, they provide further evidence that the lesions found on the Butrint and Diaporit skeletal material did not originate from a member of the MTB complex.

Consequently, the decision was then made to screen bones for the causative agents of brucellosis, since this disease produces similar lesions as skeletal tuberculosis. Two individuals from the Butrint site, burials 2722 and 4015, tested positive for brucellosis. Both of these individuals were adolescent males whose remains dated to the 11<sup>th</sup> – 13<sup>th</sup> century AD. Pathologies present on their vertebrae and ribs were very similar to one another (Figure 5). DNA extractions from bone samples produced real-time PCR products that had similar dissociation curves and melting temperatures as control DNA from *B. abortus*. Two genes were targeted in the real-time assays, IS6501 and Bscp31, with the former having a higher success rate (i.e. successful amplification).

Three rib extracts (prepared May of 2006; August of 2006, and a 1:10 dilution of an extract prepared in August of 2006) from burial 2722 were positive for IS6507. The products produced from the samples had an average T<sub>m</sub> of 80.6°C compared to the positive controls T<sub>m</sub> of 81.5. Amplification of IS6501 was also seen for two rib extracts (May of 2006 and August of 2006) and one vertebrae extract from burial 4015. A single rib and vertebra extract from burial 4015 produced positive results for Bscp31. The greater success rate of IS6501 amplification compared to Bscp31 could be because IS6501 is an insertion element and present in the genome 5 – 35 times (Ouahrani 1993). Results in this study show that both the MTB complex IS6110 and the *Brucella spp.*

IS6501 had greater success than assays for single copy genes. This provides further evidence that future assays designed to screen for pathogens would benefit from designing primers that target multi-copy elements.

Similarity of the melting temperatures between the bone extracts and *B. abortus* positive controls indicates that the same amplicon was most likely produced. These results were supported using an agarose gel, which showed that the amplicons were the same size. Both IS6501 and Bcsp31 are specific to the three members of *Brucella spp.* that are pathogenic. The amplification of these products from bone indicates that these two individuals likely had brucellosis during their lifetime. As a result *Brucella spp* is the probable causative agent behind the skeletal lesions. Osteological examination showed that the lesions of the two individuals were extremely similar and potentially caused by the same disease process. The molecular confirmation of the same pathogen in bone samples from these individuals solidifies these claims.

#### *Tuberculosis, Brucellosis, and Albania*

Both tuberculosis and brucellosis are common diseases found in modern day Albania. A study published by the WHO (2004) reported that 53 out of every 100,000 Albanians were positive for tuberculosis. A similar number of brucellosis cases were reported in 2002 with 40 out of every 100,000 Albanians having active infection. This places *Brucella spp.* infection as the number one food born illness in modern day Albania (WHO 2002). Brucellosis is such a health risk to both humans and livestock that countries worldwide, including Albania, have developed surveillance systems for the

disease. In Albania, the Ministry of Health and National Institute of Public Health require the reporting of any human positive cases, while animal infections are monitored by the Institute of Veterinary Medicine.

Incidences of these diseases in modern Albania, and the rest of Europe, have led many scientists to believe that both tuberculosis and brucellosis were present throughout the ancient Mediterranean basin. An osteological study conducted by Capasso (1999) found skeletal lesions that appeared to be consistent with brucellosis in 17.4% of adult skeletons from the town of Herculaneum. These individuals died during the eruption of Mount Vesuvius in 44 AD. *Brucella spp.* was proposed to be the causative agent behind the skeletal lesions based on gross and X-ray examination. This hypothesis was made due to similarity of the lesions to modern cases of skeletal brucellosis. Capasso (2002) also examined remnants of bacteria in preserved dairy products located at the Herculaneum site using scanning electron microscopy. The author identified several cocci-bacteria that had the appearance, size, and shape of members of *Brucella spp.* While these findings were consistent with brucellosis, other bacteria or pathogens might have been responsible for the skeletal damage. Capasso studies (1999 and 2002) confirmed that the ancient people in the Mediterranean experienced disease processes that could be consistent with tuberculosis or brucellosis. However, no molecular analysis has been performed on these remains to identify the causative agent.

The molecular data presented in this study provides concrete evidence that brucellosis was present in the ancient Mediterranean basin through the analysis of a subset of human skeletons from Butrint, Albania. Brucellosis was identified in the remains of two male adolescents from the 11<sup>th</sup> – 13<sup>th</sup> century AD. Both sets of remains

(Burials 2722 and 4015) displayed almost identical skeletal pathologies on their vertebrae. Similarities between these two individuals' age, the time period of the remains, and manifestation of the disease allow for several hypotheses regarding the history of the site as well as the health and life of its inhabitants.

The most common method of Brucellosis transmission is the ingestion of infected milk or meat from livestock (CDC 2005). A lack of pasteurization or sanitization of animal products would transmit the disease to humans. Younger individuals are more susceptible to the disease than those who acquire it later in their lifetime. Geyik et al. (2002) conducted a study in which 283 human brucellosis cases from a hospital in southeast Turkey were reviewed. The authors identified 195 individuals with musculoskeletal involvement and compared the relative ages of the patients. Out of these 195 individuals 20% were under the age of 15 years old while 63% were between the ages of 15 and 45 years old. The two individuals that tested positive in this study are close to the two age ranges where skeletal infection would be frequent. The possibility exists that the two males were fed infected meat or milk as young children and acquired an infection that progressed until their death in their early teens. Fenton (2006) stated that several other individuals were found at the site that exhibited skeletal pathologies similar to those seen in burials 2722 and 4015, during collections conducted in the summer of 2006. These individuals showed signs of minor vertebral lesions and possible healing indicating either acute infection or the ability to sustain infection more readily. Bone growth supports *Brucella spp.* infection since tuberculosis generally inhibits the process to a greater extent (Ortner and Putschar 2001). This provides support for the hypothesis that the inhabitants of the ancient site were acquiring *Brucella spp.* from

consuming livestock products. This mode of transmission continues to be common in present day Albania with the majority of brucellosis cases originating from the ingestion of infected meat or dairy in rural communities (WHO 2002).

Another possibility is that the disease was obtained from being in close contact with infected livestock. According to the Center for Disease Control and Prevention (CDC 2005) brucellosis can also be transmitted in rare cases by the handling of infected livestock or the bacterium. The CDC reports that there is a higher susceptibility to brucellosis among individuals who work with animals in general. In 1998 Wallach et al. examined an outbreak of human Brucellosis among farm workers in Argentina. According to the authors the workers had been employed on a farm where roughly 500 out of 2200 goats showed severe signs of *Brucella spp.* infection. The causative agent was later identified as *B. melitensis* and 60 workers were tested for the pathogen. Thirty-three out of sixty workers tested positive with twenty-one of these individuals having close contact with the infected herd, 11 having occasional contact and one having no contact. Studies such as these suggest that individuals employed in animal care such as veterinarians, farmers, animal handlers and laboratory workers have a higher risk of contracting the disease via close contact.

Livestock rearing and milk production are traditional economic activities in Albanian societies and even today accounts for 47% of agricultural production (Shundi 2004). Individuals involved in this field, including young males, are often required to live in close proximity of the herd and care for sick livestock. The fact that both infected individuals were adolescents could indicate that younger members of the culture worked more closely with animals in the raising, herding or care of livestock. The two young

males may have been actively involved in livestock care and as a result acquired infection due to their greater exposure to sick livestock compared to other members of the society.

A number of claims can also be made regarding the history of the site based on this molecular data. The human skeletons from Butrint and Diaporit that display lesions consistent with brucellosis come from two main time periods: the 5<sup>th</sup> – 7<sup>th</sup> Century AD and the 11<sup>th</sup> – 13<sup>th</sup> Century AD. Both of these periods can be characterized as having harsh living conditions due to the collapse of the Roman infrastructure in the late 6<sup>th</sup> century. As a result, from the 7<sup>th</sup> – 11<sup>th</sup> Century AD the region experienced a downfall in public health. In addition, the area was exposed to outside populations by the invasions of Slavic, Byzantine and Venetian cultures. A decrease in overall health and the introduction of new people may have resulted in the spread of diseases. This could include brucellosis which was molecularly confirmed in this study to be present during the 11<sup>th</sup> – 13<sup>th</sup> Century AD

The age of these remains (11<sup>th</sup> – 13<sup>th</sup> Century AD) also corresponds to the period directly before the city flooded and was ultimately abandoned. During that time the city was in ruins, the site had been subjected to centuries of war, and waters from the surrounding lakes and marshes were beginning to rise. The inhabitants of the city were mostly ‘squatters’ living in and around the ruins of the Triconch palace. It is believed that these individuals were in very poor health. Anthropological analyses of skeletal remains from the period indicate a high child mortality rate, incidences of disease, and population wide anemia and malnutrition caused by harsh living conditions (Butrint Foundation Annual Report 2004). The skeletal remains of burials 2722 and 4015 are a representation of such conditions due to the vertebral lesions and their young age at



death. The molecular identification of the causative agent centuries later would also suggest a high pathogen load. In addition, the confirmation of brucellosis suggests that the population was experiencing diseases and possibly epidemics at this time period. Malnutrition and anemia would have only accelerated the spread of pathogens and produced an increase in child mortality. Diseases such as brucellosis may have played a direct role in the downfall of the society as the waters rose and the city was finally abandoned.

The research presented here has provided novel and interesting information on remains from a World Heritage site. The identification of brucellosis in ancient Butrint contributes directly to understanding the inhabitants' health and lifestyles. Plans to conduct further anthropological and molecular research are being developed. In the summer of 2006, Dr. Todd Fenton and graduate students identified additional individuals that contained signs of skeletal pathologies. Molecular examination of these skeletal remains may lead to the identification of more individuals with brucellosis or possibly the identification of different pathogens. Additional research could also be conducted to identify which pathogenic *Brucella spp.* is present in the remains. According to Ornar and Putschar (2001) *B. melitensis* causes a greater level of bone erosion and damage than other *Brucella spp.* It is also believed that this species is common among goat populations in the Mediterranean and as a result is responsible for human brucellosis throughout the area. The molecular confirmation of *B. melitensis* in the Albanian samples would solidify these claims and provide novel information regarding both the inhabitants of Butrint and the disease process as a whole.

To the best of the researcher's knowledge this is the first time *Brucella spp.* has been identified in ancient skeletal remains. The results show how beneficial molecular identification of pathogens is to anthropological and paleopathological studies. Scientists now have the ability to identify the causative agents behind skeletal lesions. As a result, the research provides a vast amount of knowledge about the inhabitants and history of a World Heritage site. This research proved that brucellosis, as speculated, was present in the Mediterranean basin and afflicted ancient societies. It also provided knowledge on the manifestation of *Brucella spp.* infection in bone. More importantly, it indicates that brucellosis arrived to Butrint as the city was beginning to decay and may have been directly involved in its abandonment and the poor health of the inhabitants. This proves that the molecular identification of pathogens can be beneficial in understanding the lives and histories of ancient societies. Anthropologists and paleopathologists now have a new tool and ability to better understand the diseases and epidemics that have plagued mankind and ancient cultures worldwide.

APPENDIX A

**Table 21: HV1 Sequences from Individual Bone Samples.**

HV1 sequences from each bone sample (\* = indicates two separate bone extracts) compared to the Anderson et al. (1982) reference sequence. Gray regions = sequence was not obtained. Differences are noted by letters indicating the base present at that site (A-adenine, C-cytosine, T-thymine, G-guanine).

	16059	16078	16094	16103	16122	16163	16193	16199
Anderson	A	G	T	T	C	A	A	T
Burial #								
213			C					A
Bone/Primer								
Ulnar/16057			C					
Ulnar/16207			C					A
Rib/16057			C					A
Rib/16057*			C					A
Rib/16207			C					
Vert/16057								
Vert/16207								
Femur/16057				G				
Femur/16207				G				
Rib/16057								A
Rib/16057*								A
Rib/16207								
Vert/16057								A
Vert/16057*				G				A
Vert/16207								

APPENDIX A

**Table 21 (continued): HV1 Sequences from Individual Bone Samples.**

HV1 sequences from each bone sample (\* = indicates two separate bone extracts) compared to the Anderson et al. (1982) reference sequence. Gray regions= sequence was not obtained. Differences are noted by letters indicating the base present at that site (A=adenine, C=cytosine, T=thymine, G=guanine).

	16059	16078	16094	16103	16112	16163	16193	16199
Anderson	A	G	T	T	C	A	A	T
Burial #								
2722								
Bone/Primer								
Femur/16057								A
Femur/16207			C					A
Rib/16057			C					A
Rib/16207			C				C	A
Vert/16057								
Vert/16207							C	
4015								
Femur/16057								
Femur/16207								
Rib/16057								
Rib/16207								
5010								
Femur 16057						G		A
Femur 16207	T	A		C				
Rib/16057						G		
Rib/16207	T	A		C				
Vert/16057					T			
Vert/16207	T	A			T		A	

## BIBLIOGRAPHY

- Anderson, S., A.T. Bankier, B.G. Barrell, M.H.L. deBruijn, A.R. Coulson, J. Drouin, I.C. Eperon, D.P. Nierlich, B.A. Rose, F. Sanger, R.H. Schreier, A.J.H. Smith, R. Staden, and I.G. Young. 1981. Sequence and organization of the human mitochondrial genome. *Nature*. 290:457 – 465.
- Barber, A and D. Foran. 2006. The Utility of Whole Genome Amplification for Typing Compromised Forensic Samples. *Journal of Forensic Sciences*. 51: 1344 – 1349.
- Butler, J.M. 2005. Forensic DNA Typing: biology, technology, and genetics of STR markers. London: Academic Press.
- Butrint Foundation. Butrint Foundation Annual Report 2004.  
<http://www.butrintfound.dial.pipex.com/publications/ar04.pdf>. Accessed Aug 2006.
- Capasso, L. 1999. Brucellosis at Herculaneum (79 AD). *International Journal of Osteoarchaeology*. 9: 277 – 288.
- Capasso, L. 2002. Bacteria in two-millennia-old cheese, and related epizoonoses in Roman populations (abstract). *Journal of Infectious Disease*. 45:122-127
- Center for Disease Control and Prevention (CDC). Division of Bacterial and Mycotic Diseases: Brucellosis. 2005.  
[http://www.cdc.gov/NCIDOD/DBMD/DISEASEINFO/brucellosis\\_g.htm - howcommon](http://www.cdc.gov/NCIDOD/DBMD/DISEASEINFO/brucellosis_g.htm-howcommon) Accessed Aug 2006.
- Clemmer, V. 2005. Maternal Relatedness within Double Burials of an Ancient Albanian Tumulus. Thesis for Degree of M.S. School of Criminal Justice. Michigan State University.
- Donoghue, H.D., M. Spigelman, J. Zias, A.M. Gernaey-Child, and D.E. Minnikin. 1998. *Mycobacterium tuberculosis* complex DNA in calcified pleura from remains 1400 years old. *Applied Microbiology*. 27: 265 – 269.
- Drancourt, M. and D. Raoult. 2004. Molecular detection of *Yersinia pestis* in dental pulp. *Microbiology*. 150: 263 – 264.
- Edson, S.D., J.P. Ross, M.D. Coble, T.J. Parsons and S.M. Barritt. 2004. Naming the Dead: Confronting the Realities of Rapid Identification of Degraded Skeletal Remains. *Forensic Science Review*. 16: 63 – 90.
- Fenton, T. E-mail and personal communication. 7/1/2005.

- Fenton, T. E-mail and personal communication. 8/1/2006.
- Fletcher, H.A., H.D. Donoghue, G.M. Taylor, A.G.M. van der Zanden and M. Spigelman. 2003. Molecular analysis of *Mycobacterium tuberculosis* DNA from a family of 18<sup>th</sup> century Hungarians. *Microbiology*. 149: 143 – 151.
- Foran, D. R. 2006. Relative degradation of nuclear and mitochondrial DNA: an experimental approach. *Journal of Forensic Sciences*. 51: 766 – 770.
- Gehring, M. E. 2004. The Recovery and Analysis of Mitochondrial DNA from Exploded Pipe Bombs. Thesis for the Degree of M.S. School of Criminal Justice. Michigan State University.
- Geyik, M.F., A. Gur, K Nas, R. Cevik, J Sarac, and B. Dikici. 2002. Musculoskeletal involvement in brucellosis in different age groups: a study of 195 cases. *Swiss Medical Weekly*. 132: 98 – 105.
- Hall TA. 1999. BioEdit: a user-friendly biological sequence alignment editor and analysis program for Windows 95/98/NT. *Nucl. Acids. Symp. Ser.* 41:95-98.
- Hummel, S. 2003. Ancient DNA typing: Methods, Strategies, and Applications. New York: Springer-Verlag Berlin Heidelberg.
- Jaffe, H. L. 1972. Metabolic, Degenerative and Inflammatory Diseases of Bones and Joints. Philadelphia: Lea and Febiger.
- Kelley, M., and M.A. Micozzi. 1984. Rib Lesions in Chronic Pulmonary Tuberculosis. *American Journal of Physical Anthropology*. 65:381 – 386.
- Kelley, M., and M.Y. El-Najjar. 1980. Natural Variation and Differential Diagnosis of Skeletal Changes in Tuberculosis. *American Journal of Physical Anthropology*. 52:153 – 167.
- Mays, S., G.M. Taylor, A.J. Legge, D.B. Young, and G. Turner-Walker. 2001. Paleopathological and Biomolecular Study of Tuberculosis in a Medieval Skeletal Collection from England. *American Journal of Physical Anthropology*. 114:298 – 311.
- Mays, S., E. Fysh, and G.M. Taylor. 2002. Investigation of the Link Between Visceral Surface Rib Lesions and Tuberculosis in a Medieval Skeletal Series from England Using Ancient DNA. *American Journal of Physical Anthropology*. 19:27 – 36.
- Meyers, Melissa. 2006. The Utility of microbial dna and terminal restriction fragment length polymorphism analysis in the forensic examination of soil. Thesis for the Degree of M.S. School of Criminal Justice. Michigan State University.

- Misner, L. 2004. Predicting mtDNA Quality based on Bone Weathering and Type. Thesis for Degree of M.S. School of Criminal Justice. Michigan State University.
- Ortner, D.J., and W.G. J. Putschar. 1981. Identification of Pathological Conditions in Human Skeletal Remains. Washington. 29 – 52.
- O'Rourke, D.H., G. Hayes, and S.W. Carlyle. 2000. Ancient DNA Studies in Physical Anthropology. *Annual Review of Anthropology*. 29:217 – 242.
- Parra, C.A., L.P. Londono, P. Del Portillo and M.E. Patarro. 1991. Isolation, characterization and molecular cloning of a specific *Mycobacterium tuberculosis* antigen gene: identification of a species-specific sequence. *Infection and Immunity*. 59: 3411 – 3417.
- Rafi, A., M. Spielman, J. Stanford, E. Lemma, H. Donoghue, and J. Zias. 1994. Mycobacterium leprae DNA from ancient bone detected by PCR. *Lancet*. 343: 1360 – 1361.
- Rennick, S. 2005. Genetic Analysis of Monumental Structure within the Kamenica, Albania Tumulus. Thesis for the Degree of M.S. School of Criminal Justice. Michigan State University.
- Roberts, C., D. Lucy, and K. Manchester. 1994. Inflammatory Lesions of Ribs: An Analysis of the Terry Collection. *American Journal of Physical Anthropology*. 95:169 – 182.
- Sallares, R. and S. Gomzi. 2001. Biomolecular archaeology of malaria. *Ancient Biomolecules*. 3: 195 – 213.
- Shawar, R.M., F.A. el-Zaatari, A. Nataraj and J.E. Clarridge. 1993. Detection of Mycobacterium tuberculosis in clinical samples by two-step polymerase chain reaction and nonisotopic hybridization methods. *Journal of Clinical Microbiology*. 31: 61 – 65.
- Shundi, A. Country Pasture/Forage Resource Profiles: Albania. 2004. <http://www.fao.org/AG/agp/agpc/doc/Counprof/Albania/albania.htm>. Accessed December 2006.
- Sreevatsan, S., P. Escalante, X. Pan, D.A. Gilles, S. Siddiqui, C.N. Khalaf, B.N. Kreiswirth, P. Bilfani, L.G. Adams, T. Ficht, V.S. Perumaalla, M.D. Cave, J.D. Canfield and J.M. Musser. 1996. Identification of a polymorphic nucleotide in OxyR specific for Mycobacterium bovis. *Journal of Clinical Microbiology*. 34: 2007 – 2010.

- Taylor, G.M., M. Goyal, A.J. Legge, R.J. Shaw, and D. Young. 1999. Genotypic analysis of *Mycobacterium tuberculosis* from medieval human remains. *Microbiology*. 145: 899 – 904.
- Ubelaker D.H., and E.B. Jones, ed. 2003. Human remains from Voegtly Cemetery, Pittsburgh, Pennsylvania. Smithsonian Contributions to Anthropology Series, Number 46, Smithsonian Institution Press: Washington D.C.
- Uehlinger, E. 1970. Epidemiology of tuberculosis: Pathological anatomy. *Pneumology*. 143: 221 – 234.
- UNESCO. Butrint Albania: Advisory Board Evaluation. 1999. [http://whc.unesco.org/archive/advisory\\_body\\_evaluation/570bis.pdf](http://whc.unesco.org/archive/advisory_body_evaluation/570bis.pdf). Accessed Aug 2006.
- UNESCO. World Heritage Centre. 2006. <http://whc.unesco.org/pg.cfm>. Accessed Aug 2006.
- Von Endt, D.W., and D. J. Ortner. 1977. Amino acid analysis of bone in a suspected case of iron deficiency anemia. *American Journal of Physical Anthropology*. 47: 165.
- Von Endt, D.W., and D. J. Ortner. 1982. Amino acid analysis of bone from a possible case of prehistoric iron deficiency from the American southwest. *American Journal of Physical Anthropology*. 59: 377 – 385.
- Wallach, J., L.E. Samartine, A. Efron, and P. C. Baldi. 1998 "Human infection by brucella melitensis: an outbreak attributed to contact with infected goats. *FEMS Immunology and Medical Microbiology*. 19: 315 – 321.
- Wilson I. 1997. Inhibition and Facilitation of Nucleic Acid Amplification. *Applied and Environmental Microbiology*. 63: 3741 – 3751.
- World Health Organization (WHO). WHO Surveillance Programme for Control of Foodborne Infections and Intoxications in Europe: 8<sup>th</sup> Report on Albania. 2002. <http://www.bfr.bund.de/internet/8threport/CRs/alb.pdf> - [search=%22WHO%20Brucellosis%20Albania%22](http://www.bfr.bund.de/internet/8threport/CRs/alb.pdf?search=%22WHO%20Brucellosis%20Albania%22). Accessed Aug 2006.
- World Health Organization (WHO). Albania Country Profile. 2006. <http://www.who.int/countries/alb/en/>, . Accessed Aug 2006.
- World Health Organization (WHO) Albania: Tuberculosis Prevalence/Incidence. 2004. [http://www.who.int/GlobalAtlas/predefinedReports/TB/PDF\\_Files/AL\\_2004\\_Brief.pdf](http://www.who.int/GlobalAtlas/predefinedReports/TB/PDF_Files/AL_2004_Brief.pdf). Accessed Aug 2006.
- Zickel, R. and W.R. Iwaskiw. 1994. Albania: A country study, 2<sup>nd</sup> Ed. Library of Congress: Federal Research Division.



- Zimmerman, M.R., and M.A. Kelley. 1982. *Atlas of Human Paleopathology*. New York: Praeger Publishers.
- Zink, A.R., W. Grabner, and A.G. Nerlich. 2005. Molecular Identification of Human Tuberculosis in Recent and Historic Bone Tissue Samples: The Role of Molecular Techniques for the Study of Historic Tuberculosis. *American Journal of Physical Anthropology*. 126: 32 – 47.
- Zivanovic, S. Infectious and Contagious Diseases. 1982. In: *Ancient Diseases*. London: Methuen & CO: 217 – 243.